Charles University

Faculty of Science

Study programme: Analytical Chemistry

Bc. Gabriela Vlčková

Determination of the lipophilicity of fluorinated saccharides

Stanovení lipofility fluorovaných sacharidů

Master's thesis

Supervisor: doc. RNDr. Petr Kozlík, Ph.D.

Consultant: Mgr. Jindřich Karban, Ph.D.

Prague, 2025

Prohlášení:

Prohlašuji, že jsem závěrečnou práci zpracovala samostatně a že jsem uvedla všechny použité informační zdroje a literaturu. Tato práce ani její podstatná část nebyla předložena k získání jiného nebo stejného akademického titulu.

V Praze, *05.05.2025*

Podpis

Abstrakt

Tématem této diplomové práce je stanovení lipofility fluorovaných β-methyl glykosidů disacharidu D-laktosy (laktosidů) a vývoj vhodných analytických metod pro tento účel. Lipofilita byla nejprve stanovena přímou metodou termodynamického rozdělení zkoumané látky mezi vodu a n-oktanol. Hodnoty dekadických logaritmů rozdělovacích koeficientů zkoumaných látek (log *P*) byly vypočteny z integrálních intenzit jejich ^{19}F NMR signálů v n-oktanolové a vodné fázi.[1] Následně byla vyvinuta alternativní metoda stanovení relativní lipofility jednotlivých laktosidů, založená na porovnání retenčních časů získaných hydrofilní interakční kapalinovou chromatografií (HILIC). Jako detekční metoda byla zvolena vysoce rozlišená hmotnostní spektrometrie (HRMS). Hodnoty získané metodou ^{19}F NMR byly porovnány s novou HILIC metodou a byla hodnocena použitelnost postupu HILIC-HRMS pro stanovení lipofility deoxyfluorovaných sacharidů. Experimentálně získané hodnoty log *P* byly také porovnány s hodnotami predikovanými metodou COSMO-RS. Stanovení metodou termodynamického rozdělení poskytlo výsledky v dobré shodě s výpočetní predikcí, zatímco metoda HILIC-HRMS poskytla u některých látek výsledky rozdílné.

Klíčová slova: *fluorované sacharidy, log P, NMR spektroskopie, HILIC, MS spektrometrie, COSMO-RS*

Abstract

The topic of this master's thesis is determining the lipophilicity of fluorinated β-methyl glycosides of the disaccharide D-lactose (lactosides) and developing suitable analytical methods for this purpose. Lipophilicity was first determined by the direct method of thermodynamic partition of the investigated substance between water and n-octanol. The values of the decadic logarithms of the partition coefficients of the studied substances (log *P*) were calculated from the integral intensities of their ^{19}F NMR signals in the n-octanol and aqueous phases.[1] Subsequently, an alternative method for determining the relative lipophilicity of individual lactosides was developed, based on the comparison of retention times obtained through hydrophilic interaction liquid chromatography (HILIC). High-resolution mass spectrometry (HRMS) was selected as the detection method. The values obtained by the ^{19}F NMR method were compared with those derived from the new HILIC method, and the applicability of the HILIC-HRMS procedure for determining carbohydrate lipophilicity was evaluated. Experimentally obtained log *P* values were also compared with values predicted by the COSMO-RS method. The thermodynamic partitioning method provided results that were in good agreement with computational predictions, while the HILIC-HRMS method produced varying results for some substances.

Key words: *fluorinated carbohydrates, log P, NMR spectroscopy, HILIC, MS spectrometry, COSMO-RS*

Content

Used abbreviations

ACN	Acetonitrile
ADMET	Absorption, Distribution, Metabolism, Excretion and Toxicology
ATP	Adenosine triphosphate
CAD	Charged Aerosol Detector
COSMO-RS	COnductor like Screening Model for Real Solvents
d	doublet
dd	doublet of doublets
ddd	doublet of doublet of doublets
DFT	Density Functional Theory
DNA	Deoxyribonucleic acid
ELSD	Evaporative Light Scattering Detector
ESI	Electrospray ionization
FD	Fluorescence detector
HILIC	Hydrophilic Interaction Liquid Chromatography
HPLC	High Performance Liquid Chromatography
HRMS	High Resolution Mass Spectrometry
LacNAc	Methyl *N*-acetyl-β-D-lactosaminide
Lac	Methyl β-D-lactoside
m	multiplet
mp	melting point
m/z	mass-to-charge ratio
NMR	Nuclear Magnetic Resonance
NS	Number of Scans
PDA	Photodiode Array Detector
PE	Petroleum Ether
QSAR	Quantitative Structure-Activity Relationship
QSPkR	Quantitative Structure-Pharmacokinetic Relationship
qNMR	quantitative Nuclear Magnetic Resonance
RNA	Ribonucleic acid

RSD	Relative Standard Deviation
SD	Standard Deviation
S/N	Signal-to-Noise ratio
TLC	Thin Layer Chromatography
UHPLC	Ultra-High-Performance Liquid Chromatography
UV	Ultraviolet light
VIS	Visible light

1. Introduction

Lipophilicity is an important property of organic compounds and a significant parameter in the development of novel therapeutics.[2] Introducing fluorine into a molecule is a common approach to modulate the pharmacological properties of biologically active substances, including lipophilicity.[3] It is also one option for preparing glycomimetics – substances that mimic the structure and functions of carbohydrates.[4,5,6] Glycomimetics are frequently designed to affect biological processes associated with specific carbohydrates, contributing to the development of new drugs and diagnostic methods.[7]

Lipophilicity of a substance is often expressed as the decimal logarithm of its partition coefficient between n-octanol and water (log *P*). Organic solvent (n-octanol) closely simulates the properties of lipid membranes in cells, while water represents the polar (aqueous) environment in the human body.[8] Although concentrations in both phases are commonly determined using UV spectroscopy, this method does not apply to carbohydrates because they lack chromophores, necessitating alternative approaches.

2. State of the Art

2.1 Structure and Function of Carbohydrates

Saccharides, also known as carbohydrates, are essential biomolecules that play an important role in various biological processes, such as cell growth and energy metabolism. They are found in all organisms where they have important functions. They are often part of other important molecules such as DNA, RNA, ATP, etc. On the other hand, given their involvement in living organisms, they are also inevitably connected to the development of diseases such as cancer.[6] They are often classified into three main types: monosaccharides, oligosaccharides, and polysaccharides.[9] Monosaccharides, such as D-glucose, D-fructose, or D-galactose, are the simplest form of carbohydrates. They usually appear as colorless, crystalline, and water-soluble compounds that are rapidly absorbed by the human intestines. The most important carbohydrate in terms of energy metabolism is D-glucose, because it provides immediate energy to the human body.[9,10,11] Monosaccharides can be further divided according to two criteria: by the number of carbon atoms (pentose, hexose, etc.) or by the position of the carbonyl group in their structures (aldoses or ketoses). The classification of monosaccharides into the D- or L-series is determined by the orientation of the hydroxyl group on the chiral carbon furthest from the carbonyl group in the Fischer projection. This classification is based on the configuration of glyceraldehyde, the simplest chiral carbohydrate, which serves as a reference point. If the configuration at the most distant chiral carbon atom (termed the configurational atom) matches the configuration of D-glyceraldehyde (with the hydroxyl group pointing to the right in the Fischer projection), the carbohydrate belongs to the D-series. Conversely, if it matches the configuration of L-glyceraldehyde (with the hydroxyl group pointing to the left in a Fischer projection), the carbohydrate belongs to the L-series. Reducing pentoses and hexoses undergo an intramolecular cyclization reaction in solutions to form pyranose or furanose rings. This process creates a new stereogenic center – an anomeric carbon. To indicate the configuration of substituents on the anomeric carbon, we use the symbols α- and β-, which denote the relative configuration in relation to the anomeric reference atom: the exocyclic oxygen atom at the anomeric center in the α-anomer is formally *cis*, in the Fischer projection, to the oxygen attached to the anomeric reference atom**,** while the β-anomer has formally *trans* configuration. The anomeric reference

atom is identical with the configurational atom for the majority of simple monosaccharides. Monosaccharides are the building blocks for more complex oligosaccharides and glycoconjugates.

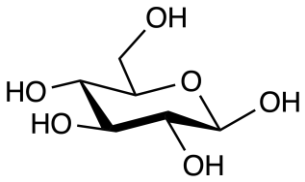

Figure 1: β-D-glucose

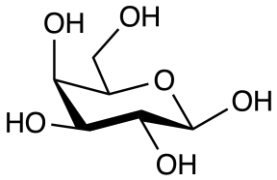

Figure 2: β-D-galactose

Oligosaccharides are structurally complex saccharide polymers consisting of two to about ten monosaccharide units. They are formed by the combination of monosaccharides through a glycosidic linkage created by a glycosylation reaction. Among the most common oligosaccharides are disaccharides D-sucrose (composed of D-glucose and D-fructose) and D-lactose (consisting of D-galactose and D-glucose). Disaccharides can be categorized into two types: reducing disaccharides, where one of the two monosaccharides retains its free hemiacetal function at the anomeric atom and can act as a reducing agent, and non-reducing disaccharides, in which the component monosaccharides are linked through an acetal linkage between their anomeric centers. Disaccharides are broken down into monosaccharide units by the corresponding enzymes in the intestines. These resulting monosaccharides are then used in biochemical processes in the human body, such as Krebs cycle.[9–11]

Polysaccharides are long chains of monosaccharide units linked together by glycosidic linkage. Examples include starch, glycogen, and cellulose. Polysaccharides serve as energy storage (starch in plants and glycogen in animal and fungal cells) or structural components (cellulose in plant cells), and some of them also participate in cellular recognition. During the process of digestion, polysaccharides are cleaved to monosacharides. For example, molecules of starch are cleaved to D-glucose, which can be utilized in glycolysis, etc.[9]

Oligosaccharides and polysaccharides are the carbohydrate parts of glycoconjugates (glycoproteins, glycolipids) and are commonly referred to as glycans. Glycans bind to various proteins and play a key role in many biological processes, including embryogenesis, immunity, inflammation, and cancer.[12] Recognition of glycans is important for cell-to-cell communication, allowing immune cells to distinguish between self and non-self cells.[5] In the past few years, glycan binding has become an interesting topic and target to many researchers, due to its potential in new drug development.[4]

Oligosaccharides typically exhibit low affinity to their cognate protein receptors and only mediocre stability *in-vivo*. To overcome these drawbacks of naturally occurring carbohydrates, their synthetically modified analogs are frequently developed.[13] These compounds, referred to as glycomimetics, imitate the structure and function of naturally occurring carbohydrates while offering enhanced pharmacokinetic properties.[14]

2.1.1 Fluorinated saccharides

Fluorinated carbohydrates are a class of compounds in which fluorine has been introduced into a molecule. A subgroup of fluorinated carbohydrates is known as deoxyfluorinated carbohydrates, where one or more hydroxyl groups in a carbohydrate molecule are substituted with fluorine atoms. Due to the similarities of fluorine and oxygen in terms of their Van der Waals radii and electronegativities, the C-F bond is comparable in size and polarization to the C-OH bond. The C-F bond has high dissociation energy, which often makes fluorinated compounds less prone to metabolic transformations.[15] Even though fluorine isn't usually part of naturally occurring molecules, more than one-third of new small-molecule pharmaceutics are fluorinated.[5] This modification significantly alters the physical, chemical, and biological properties of the original carbohydrate, including lipophilicity and metabolic stability.[4] The introduction of fluorine atoms into carbohydrate structures can be achieved through several methods, including nucleophilic fluorination, electrophilic addition, radical reactions, etc.[16]

Fluorinated saccharides have shown potential in numerous biological applications. For instance, they are used as chemical probes to study molecular recognition of natural glycans.[6] Their enhanced stability against enzymatic degradation makes them great candidates for synthetic vaccines[17] and immunogens.[18] The absence of fluorine in biological macromolecules makes fluorinated saccharides an outstanding bioanalytical probes for the study of kinetic

transport phenomena, lectin*–carbohydrate interactions or for in vivo imaging of tumors and drug distribution.[6] For example, a glucose analog labeled with the radioactive isotope fluorine-18, (^{18}F)-2-deoxy-2-fluoro-D-glucose, is the most common radiotracer in positron emission tomography (PET) imaging, with an important applications in cancer diagnostics, cardiology or neuroimaging.[19]

2.2 Lipophilicity

Lipophilicity (sometimes also hydrophobicity) is one of the most studied physical properties of compounds with biological activity.[20] The term comes from the Greek: "lipos" (fat) and "philos" (friendly). Lipophilic compounds are able to dissolve, be dissolved in, or absorb lipids. Lipophilicity is typically expressed as the ratio of the concentrations of a compound in a mixture of two immiscible solvents at equilibrium, called partition coefficient (*P*).[21] In chemistry, pharmacology or toxicology, lipophilicity is one of the essential parameters of biologically active compounds, affecting their absorption, distribution, metabolism, excretion and toxicity (ADMET).[22, 23]

The cell membrane is a dynamic structure forming the boundary between the inside of the cell and its external environment. It is essential for maintaining cellular integrity and regulating the transport of substances into and out of the cell. The cell membrane consists of a bilayer of phospholipids, molecules with a hydrophilic head and hydrophobic tail. The hydrophobic tails of the phospholipids face inward into the bilayer, forming a hydrophobic center, while the hydrophilic heads face outward.[24] To successfully cross the cell membrane, the potential drug must not only enter the membrane, but it also has to come out the other side. Very hydrophilic drugs enter the membrane with great difficulty, which leads to poor ADMET properties, while overly lipophilic substances can accumulate in the membrane, potentially leading to *in vivo* toxicity.[25] Therefore, a certain balance between lipophilicity and hydrophilicity is ideal for crossing the cell membrane, although lipophilic substances generally tend to cross the lipid bilayer more easily than hydrophilic ones.[2]

*Lectins are a large group of non-immune proteins that can recognize and bind sugars with a high degree of specificity.

In addition, knowledge of lipophilicity is essential in environmental chemistry[26] because it determines the distribution of chemicals in the environment, and in cosmetology[27] because it affects the penetration of active ingredients through the skin.

The partition coefficient (*P*) is commonly used to quantify the lipophilicity of a molecule. It is defined as the ratio of the concentrations of the substance at equilibrium in a two-phase system, partitioning between an organic solvent (such as n-octanol) and water.[28] The organic solvent is used to model the cell membrane.[8] The most commonly used is n-octanol because its structure is similar to the components of the cell membrane, however, other organic solvents can be used as well (e.g. cyclohexane, chloroform, propylene glycol).[29] The partition coefficient can be calculated using the following formula, where c_o is the concentration of compound in organic phase and c_w is the concentration of the compound in water phase.

$$P = \frac{c_o}{c_w} \tag{1}$$

The partition coefficient is frequently expressed as log *P* because it provides a more manageable scale for representing the wide range of partition coefficients.[30] As a quantifier of lipophilicity, it is one of the key determinants of the physicochemical properties of drugs and industrial chemicals. It has become one of the main parameters used in investigations of quantitative relationships between the chemical structure of a substance and its biological activity (QSAR),[28] or pharmacokinetic properties (QSPkRs).[20]

In the literature, we can often find log *D* values for lipophilicity expression. The difference between log *P* and log *D* is that log *P* describes the partition equilibrium of an unionized solute between water and an immiscible organic solvent, while log *D* is a pH dependent lipophilicity value that determines the ratio of the sum of the concentrations of all forms of the compound between both phases.[31] The log D can be calculated using the following formulas:[20]

$$\log D_{acid} = \log P + \log\left[\frac{1}{\left(1+10^{pH-pK_A}\right)}\right] \tag{2}$$

$$\log D_{base} = \log P + \log\left[\frac{1}{\left(1+10^{pK_A-pH}\right)}\right] \tag{3}$$

According to Lipinski's Rule of 5, an orally taken molecule has a good chance of being well absorbed to systemic circulation if the log *P* value is less than 5, there are less than 5 hydrogen bond donors, and less than 10 hydrogen bond acceptors in its structure.[32] However, recent studies show that the optimal lipophilicity value lies within a range of log *P* = 1–3 to ensure optimal physiochemical properties.[20, 2]

Carbohydrates are generally considered to be highly polar molecules with very low lipophilicity, due to the presence of a number of hydroxyl groups in their structures.[33] However, the lipophilicity of carbohydrates can be increased by replacing a hydroxyl group with a fluorine atom (deoxyfluorination), as discussed above.[4]

2.2.1 Methods for the Determination of Lipophilicity

The log *P* values can be determined experimentally using various methods. In general, we could divide them into direct and indirect.[34] Direct methods typically rely on thermodynamic partitioning of the analyte in the n-octanol/water two-phase system and subsequent determination of its concentrations in both phases. These include the “shake-flask” method, "stir-flask" method and two-phase titrations.[35]

The shake-flask method represents a traditional, well-known procedure for determining the lipophilicity of the analyte. The compound of interest is introduced into a separation funnel containing both water and the organic solvent. The separating funnel is shaken long enough to achieve equilibrium partitioning of the compound between the two phases. The phases are then separated and the concentration of the analyte in each phase is determined by an appropriate analytical technique, such as UV/VIS spectroscopy or HPLC with suitable detection,[31,36] providing the log *P* value. The method is time-consuming, requires a large amount of pure compound and its application is limited to compounds having log *P* values in the following range (ca. $-3 < \log P < 4$). Outside this range, the obtained values are unreliable.[37]

The stir-flask method was developed from the shake-flask method, but instead of shaking, the two-phase system is stirred for the necessary time until equilibrium is established. With this method, there is a lower risk of emulsion formation than with the shake-flask method.[31,35]

Potentiometric titration is used to measure changes in electric potential during the titration of a substance that is partitioned between water and a non-polar organic phase. This method can be applied to molecules that can undergo facile protonation or deprotonation. The measurement of the potential is dependent on the changes in the concentration of ions that occur during the titration, which enables the calculation of the concentrations of the substance in the individual phases. The dissociation equilibria in the aqueous phase are expressed by the pK_a values of the molecule while the overall dissociation equilibria regarding the whole system is described by the apparent pK_a (pK_a ^{app}). The pK_a and pK_a^{app} values can be determined by the titration of the compound in the biphasic system and in the aqueous phase. Log *D* value of particular compound can then be calculated from its pK_a and pK_a^{app} constants.[38]

Indirect methods rely on empirical linear correlation between the partition coefficient and other partitioning phenomena (equation 4).[35] The value of log *P* is typically determined by correlating a compound's retention properties in a reverse-phase chromatographic system with its partition coefficient. This correlation can be described with equation:

$$\log P = a \log k + b \tag{4}$$

In the above equation, *k* is an expression for the retention factor, which can be calculated from the retention times or as the ratio of the average number of molecules of the substance in the stationary phase (n_s) and the mobile phase (n_m) during the measurement:

$$k = \frac{n_s}{n_m} = \frac{t_R - t_0}{t_0} \tag{5}$$

Where t_R is the measured retention time of the substance and t_0 is the dead retention time.[39] The retention factor is used to evaluate lipophilicity in logarithmic form – log *k* (equation 4). First, samples with known log *P* values are analyzed. This determines the terms *a* and *b* of the equation 4, which allows the log *P* to be determined for other samples. In the case of measurement by thin layer chromatography, the log *k* value in equation 4 is replaced by the R_M value (equation 6).[40] Chromatographic methods are used mostly because they require a very

small amount of sample, are relatively fast and can be automated. They are also not as demanding on the purity of the sample.[41]

The reverse–phase HPLC for lipophilicity measurements is based on measuring the retention times of substances. The retention time directly depends on the distribution of the substance between the stationary and mobile phase. As mentioned above, this method can be used when a series of standards, with known log *P*, are first injected on the column and the retention times are used for the calibration curve. The retention time of the tested compound is then compared to the calibration curve and its log *P* is determined (equation 4).[42]

The RP-TLC method is probably the easiest chromatographic method that can be used for lipophilicity determination. It uses measured R_f values and calculated R_M values to evaluate the lipophilicity of substances.[41]

$$R_M = \log\left[\left(\frac{1}{R_f}\right) - 1\right] \tag{6}$$

where R_f is the retention factor which is the ratio of the distance travelled by solute to the distance travelled by solvent. The value of R_M is inversely proportional to R_f.

Similarly, as the HPLC method, the capillary electrophoresis (CE) method also uses the log *k* parameter to evaluate lipophilicity. This method separates molecules based on their different partition coefficients between aqueous and micellar phases.[42]

In vitro ADMET properties such as log *P,* solubility and permeability through membranes can also be predicted by computational approaches without the need for experimental measurements. The most commonly used methods are empirical, which typically use machine learning algorithms that optimize models using a training set of molecules with known log *P* values. To generate high-quality predictive models, it is necessary to use a training set of compounds with great structural diversity.[42] Other commonly used predictive approaches include fragment methods, in which log *P* is estimated based on contributions from individual fragments of the molecule[43], or quantum mechanical methods using electronic structure calculations.[44] Quantum mechanical methods also include COSMO-RS approach, which is discussed in more detail below. Predicting ADMET properties is essential in drug discovery,

allowing optimization of drugs' pharmacokinetic properties without excessive experimental testing.[32]

2.3 NMR spectroscopy

NMR (nuclear magnetic resonance) spectroscopy is an amazing tool for the structural analysis of molecules. It has become indispensable in research and analysis in chemistry, biology, and medicine.[45,46] NMR is a non-destructive method enabling the measurement of various nuclei. NMR is commonly used for measurement of proton (^{1}H), carbon (^{13}C), nitrogen (^{15}N) fluorine (^{19}F) or phosphorus (^{31}P) nuclei as these elements have sufficient natural abundance of isotopes with magnetic moments μ and spin number of I = ½, interacting with a magnetic field. Conversely, nuclei with a spin number of I = 0, such as ^{12}C and ^{16}O, have an even number of protons and neutrons, which means that they don't have a magnetic moment, and they can't be measured with NMR. Nuclei with spin number I greater than ½ have both a magnetic moment and an electric quadrupole moment, which makes them difficult to measure.[47]

If we place a nucleus with a non-zero magnetic moment in a strong magnetic field, the energy levels of its nuclear spins will split. According to the laws of quantum mechanics, nucleus with I = ½ can only be permanently at one energy level and therefore, the spin can only have one of two possible orientations. The difference in energy between these two states depends on the strength of the magnetic field and the type of nucleus. The populations of nuclei on both energy levels are almost the same. There is only a slightly larger number of nuclei at the lower energy level than at the higher energy level. This ratio of nuclei can be calculated using Boltzmann's distribution:

$$\frac{N_\alpha}{N_\beta} = e^{\Delta E/k_b T} \tag{7}$$

Where k_b is a Boltzmann constant, T is thermodynamic temperature and ΔE is a differential between spin energy of α and β. The vector sum of all nuclear magnetic moments is called the magnetization, M_0. Because the level difference ΔE is small, the total magnetization is small and the resulting NMR signal is weak.[48,49] If the nuclei is subsequently exposed to a radiofrequency (RF) irradiation with an energy corresponding to the energy difference ΔE, part of the nuclei at lower energy level will absorb the radiation and move to a higher energy level.

As a result, the population of nuclei at both energy levels is equalized. This causes the sample magnetization M_0 to move from its equilibrium position. Once the RF irradiation stops, the excited nuclei will subsequently "relax" back to a lower energy level.[50]

We distinguish two types of relaxation processes:

- Spin-lattice (longitudinal) relaxation (T_1): restoration of equilibrium magnetization in the magnetic field direction (in the z axis). T_1 time is the time required for the nucleus to return energy back to the surroundings.[48]
- Spin-spin (transverse) relaxation (T_2): reduction of magnetization in the xy plane by mutual interaction of neighboring nuclei. With a shorter T_2 time, the magnetization reduces faster.[48]

One of the most important aspects of NMR spectroscopy is the chemical shift δ, which is the shift of the resonance of nuclei relative to the reference compound in a magnetic field. The chemical shift of a nucleus depends on its chemical environment. The nuclei of atoms are shielded by the surrounding electrons, which create a magnetic field that has the opposite direction to the external magnetic field. Nuclei of the same isotope can, therefore, be differently shielded by electrons, which leads to different chemical shifts. Nuclei that are more shielded have a lower chemical shift and vice versa. Nuclei that have the same chemical environment are called chemically equivalent; they are shielded with electrons the same way, and therefore they have the same chemical shift. This chemical shift is measured in ppm (parts per million) and provides important information about the chemical environment and the structure of the molecule. Chemical shift is defined as follows:

$$\delta_x = 10^6(\upsilon_x - \upsilon_{ref})/\upsilon_{ref} \tag{8}$$

Where δ_x is a chemical shift of atom *x,* υ_x is a resonant frequency of atom x and υ_{ref} is a resonant frequency of reference compound.[47,48]

Another important phenomenon observed in NMR spectra is spin-spin coupling (*J*-coupling), which manifests itself as a signal splitting. This effect is caused by the interaction between electrons and nuclei and occurs when the spin of one nucleus affects the spin of a neighboring nucleus, causing a splitting of signals in both nuclei involved. Spin-spin coupling provides information about the molecule's structure.[49]

2.3.1 ^{19}F NMR

As already mentioned, fluorine nuclei are commonly measured by NMR spectroscopy. Fluorine has 100% abundance of NMR active isotope ^{19}F and a large gyromagnetic ratio, which causes a relatively high sensitivity (approximately 83% of ^{1}H NMR sensitivity).[51] Another advantageous property is that the chemical shifts of fluorine cover a wide range (about 900 ppm), which usually results in good signal separation and facile interpretation of the NMR spectrum. Pure trichlorofluoromethane ($CFCl_3$), which has a chemical shift of 0 ppm, is most commonly used as a reference compound.[52]

Since all ^{19}F nuclei are magnetically active, *J*-coupling with neighboring magnetically active nuclei splits ^{19}F NMR signals into multiplets. This *J*-coupling usually occurs through 1-3 bonds but long-range coupling through multiple bonds was also observed, especially in conjugated or aromatic systems.[48] *J*-coupling between two fluorine atoms can reach values up to 300 Hz, which is caused by the large ^{19}F gyromagnetic ratio. *J*-coupling observed between fluorine and hydrogen is usually larger than in the case of two hydrogen nuclei.[48]

2.3.2 Log *P* determination

Although NMR spectroscopy is not as widely used for the determination of *in vitro* ADMET properties as other analytical methods such as high-performance liquid chromatography (HPLC), it is still an important part of the development of new drugs. NMR is commonly employed for structural analysis of new substances, including drugs. In addition, quantitative NMR (qNMR) can also be used for determining the concentrations of analytes.[45]

Quantitative NMR measurements can be divided into two types – absolute and relative. The absolute method is more accurate, but also more difficult to perform. In this method, the intensity of the integral of the measured compound is compared to the intensity of the integral of a standard (calibration compound) of known concentration. From that information, we can further derive the absolute concentration of the substance. To perform this method, it is important to weigh all of the compounds as accurately as possible. Relative measurements are more commonly used than absolute methods because of its simplicity. This method does not require precise weighting because it compares only the ratio of two integrals – standard and

analyzed compound. Relative measurements can be used for example in log *P* determination (details described below).[53,54]

In order to make a quantitative NMR experiment as accurate and reproducible as possible, it is necessary to set all parameters and choose a suitable signal carefully. The signal should be as simple as possible (singlet is superior to multiplet, etc.) with none or minimal overlap with other signals. The key parameter is a sufficient delay between individual scans (d_1), which must be at least five times the longitudinal relaxation time T_1 to ensure complete magnetization relaxation between individual pulses. The homogeneity of the magnetic field must be optimized (shimming) to minimize peak broadening and to achieve maximum spectral resolution. The number of scans should be high enough to achieve the desired signal-to-noise ratio (S/N), of at least 250:1 for good measurement accuracy. The spectral width must encompass the full range of chemical shifts, with a minimum extension of 10% of space on each side to prevent signal attenuation. Transmitter frequency offset should also be set in the proximity of all signals evaluated to ensure their uniform excitation. The spectrum processing (baseline correction, phasing, etc.) is also very important.[53,55]

As previously noted, various methods exist for determining lipophilicity; however, not all are suitable for specific molecules like carbohydrates, which do not have chromophores. In such instances, alternative techniques like NMR become necessary, as they do not depend on chromophores and enable direct analyte detection. Several strategies can be utilized for log *P* assessment using ^{1}H NMR spectroscopy. For example, an article by Mo et al. describes a method for determining the partition coefficient of pharmaceuticals between octanol and water using NMR spectroscopy without the use of deuterated solvents.[56] This technique eliminates the need for deuterated solvents and reference substances, which simplifies and accelerates the experimental procedure.[56] Soulsby and co-workers combined the determination of partition coefficient using ^{1}H NMR spectroscopy with time domain complete reduction to amplitude-frequency tables (CRAFT).[57] This technique provides amplitudes of specific signals without the need for Fourier transformation, avoiding problems with phasing, baseline correction and internal standardization. Miniature shake-flask method in NMR tube for octanol-water partition coefficient determination was described by Rücker.[58] In this procedure NMR data of the initial

concentration in water are measured first. After that, extraction with octanol takes place in NMR tube and the bottom water layer is measured again with ^{1}H NMR spectroscopy.

Incorporating fluorine into carbohydrates alters their physicochemical properties, such as lipophilicity. The presence of fluorine in molecule also enables to determine log *P* with the use of ^{19}F NMR spectroscopy. This technique was recently established by Linclau and colleagues, utilizing the partitioning of the analyte alongside a fluorine-containing standard with a predetermined log *P* value between water and octanol. After equilibrium is reached, both phases are taken into an NMR tube and analyzed with ^{19}F NMR spectroscopy.[1]

2.4 Hydrophilic Interaction Liquid Chromatography

Hydrophilic Interaction Liquid Chromatography (HILIC) was first introduced by Andrew J. Alpert in 1990.[59] This chromatographic technique serves as an alternative to Normal Phase Liquid Chromatography (NP-LC), primarily for the separation of polar compounds. The stationary phase in HILIC is typically composed of silica gels coated with polar organic functions such as amino groups or diols. For example, aminopropyl functionalized silica gel can be coated with polysuccinimide and subsequently derivatized with 2-aminoethanol providing commonly used poly-[(N-hydroxyethyl)-aspartamide] stationary phase. The stationary phases are either neutral (amide, diol, cyclodextrine), charged (modified silica gel), or zwitterions (sulfobetaine). The mobile phase contains a high percentage (> 60 %) of an aprotic organic solvent miscible with water (usually acetonitrile), and a smaller proportion of an aqueous phase.[60] To ensure appropriate mobile phase properties (such as pH and ionic strength), buffered solutions containing ammonium acetate or ammonium formate are commonly used.[61] The pH and ionic strength of the mobile phase generally influences ionization of both the analytes and the functional groups of the stationary phase, affecting the retention of analytes. The significance of these effects depends on the stationary phase used and the acid-base properties of the analyte.[62] Another important factor for achieving efficient separation and suitable peak shapes is the selection of an appropriate sample solvent. The sample solvent must have a similar or even identical composition compared to the mobile phase.[60]

The separation mechanism on the HILIC column is still not fully understood.[60] One of the proposed mechanisms describing HILIC separation is based on the formation of an aqueous layer on the surface of the stationary phase, creating a liquid-liquid extraction system. This causes the retention of polar compounds on the stationary phase.[63] Therefore, the mobile phase must contain at least 3% water to keep the stationary phase hydrated.[64] Several factors contribute to the retention mechanism on a HILIC column, including hydrogen bonding, ionic interactions or hydrophobic interactions.[61,64] In general, polar analytes interact strongly with the stationary phase, resulting in their slow elution. In contrast, non-polar compounds pass rapidly through the column, due to the absence of these polar interactions. The composition of the mobile phase has a great influence on analyte retention. The retention of a polar analyte can be reduced by increasing the polarity of the mobile phase. Although water is most commonly used as the polar component of the mobile phase, in some cases it can be partially or fully replaced by another solvent, such as methanol or ethanol.[60]

HILIC is widely used in the pharmaceutical industry, medical sciences or proteomics for the separation and analysis of biologically active substances, such as amino acids, carbohydrates or nucleotides. HILIC separations have gained popularity in part because of their ease of combination with a variety of detection techniques, including ultraviolet light absorption (UV), fluorescence (FL), evaporative light scattering (ELSD), refractive index (RI) or mass spectrometry (MS).[61]

2.4.1 HILIC-ESI-MS

The HILIC separation technique is compatible with electrospray ionization mass spectrometry detection (ESI-MS). This is due to the possibility of using volatile mobile phases consisting of acetonitrile and ammonium salt-based buffers.[61,65] Electrospray ionization (ESI) is a soft ionization technique that uses an electrospray in which a high electrical voltage is applied to transfer analytes from the liquid phase to an aerosol without significant fragmentation. As the liquid droplets move towards the mass spectrometer, the solvent evaporates until the droplets reach the Rayleigh limit, when electrostatic repulsive forces overcome the surface tension of the liquid. This is followed by a Coulombic explosion – the disintegration of the droplet into smaller, more stable particles. These ions are then transferred to the mass analyzer using electric fields, where they are separated based on their mass-to-charge ratio (m/z).[66] In comparison to

normal phase chromatography, the sensitivity of ESI-MS detection is in HILIC increased due to the use of a mobile phase with a higher content of polar components.[65]

The combination of HILIC separation with MS detection finds application where reversed-phase chromatography (RP-HPLC) cannot be used – in the separation of highly polar compounds. The advantages of this combination are high sensitivity, good reproducibility and the possibility of analyzing complex biological matrices with minimal sample preparation. On the other hand, the optimization of the separation conditions can be more demanding, especially when choosing the ideal mobile phase.[65]

2.5 Development and optimization of the HPLC method

Developing and optimizing an HPLC method involves several important steps to achieve accurate and reproducible results. The parameters that need to be included when developing a method are: the physicochemical properties of the analyte, selection of chromatographic conditions, sample preparation and method optimization.[67]

2.5.1 Determination of physicochemical properties of the analyte

Identifying the physicochemical properties of an analyte is usually the first step in method development and optimization, prior to further steps such as selecting a separation or detection method. These properties include molecular weight, solubility, polarity, acid-base properties, and stability.[68] It is also important to determine the goal of the developed method, such as the requirement for sensitivity and speed of the method, etc.[67]

2.5.2 Selection of chromatographic conditions

Selection of the appropriate column for HPLC analysis is essential to achieve effective separation of analytes. Analytes can be categorized according to their physicochemical properties, such as solubility, polarity, and molecular weight. This categorization allows us to select an appropriate chromatographic method. For most determinations, silica gel or modified silica gel is a suitable stationary phase. However, if analysis at higher temperatures is required, other stationary phases such as hybrid or polymeric can be selected instead.[67] The next step is to choose the separation mechanism. If the analyte is polar, normal-phase chromatography or HILIC is often the method of choice, whereas for non-polar substances, reversed-phase

chromatography is more appropriate.[68] For ions and ionizable molecules such as proteins, ion exchange chromatography is suitable. Separation by molecular size, for example for polymers, is performed by gel permeation chromatography.[67]

As follows from Van Deemter's theory, particle and pore size affect the efficiency of chromatographic separation.[60] The standard particle size for conventional HPLC is 3-5 μm, while particles smaller than 2 μm are used for UHPLC. The pore size of the column is selected according to the molecular weight of the analyte. Usually, a pore size of 100 Å is used for smaller analytes (M < 10 000 g/mol) and 300 Å for larger (M > 10 000 g/mol). The length and diameter of the column affect the resolution and analysis time. Longer columns provide better resolution but increase analysis time and consumption of the sample and solvent.[67,69]

The selection of the mobile phase depends on all the factors mentioned above. It influences the solubility and separation of analytes. The choice of mobile phase varies for a particular chromatographic system, for example:

- For HILIC setup, a typical mobile phase is a mixture of ACN and water with the addition of buffer (e.g. ammonium acetate).
- For NP-HPLC, binary mixtures with different polarity are used most often – an aliphatic hydrocarbon and a polar component of the mobile phase (e.g. propanol).
- In RP-HPLC, the mobile phase is polar – usually water or buffers mixed with polar organic solvents such as alcohols.[69]

2.5.3 Selection of detector

Another important factor is the choice of detector. This choice again depends on the nature of the analyte, but also on the desired detection limit and sensitivity. The most commonly used detectors include UV, PDA, FD, ELSD, CAD, and MS.[70] There are many requirements to consider when selecting the appropriate HPLC detector, and none of the detectors fulfills all of them. The limitation of using UV/VIS/PDA detectors is that the analyte must have a chromophore, and the mobile phase must transmit the selected wavelength.[67] On the other hand these detectors are nondestructive, reliable, inexpensive, and easy to use, which makes them the most widely used. Fluorescence detectors (FD) are highly sensitive, but there are not many compounds with fluorescence properties. Light scattering detectors (ELSD) are very universal

but require the use of a volatile mobile phase and they are also not very sensitive. Charge aerosol detectors (CAD) are universal and just like ELSD require the use of volatile buffers.[70,71] The connection of HPLC with MS spectrometry ensures high sensitivity, selectivity, and reliability. However, the use of volatile mobile phase is necessary.[67]

2.5.4 Sample preparation

The preparation of sample affects all of the following steps, which makes it probably the most important and also time-consuming step in the whole process.[72] The entire sample preparation involves a few equally important steps—every operation performed with the sample before its determination is considered "sample preparation".[73] The first important step is sample collection, which usually follows standards and regulations and differs for different states of matter.[74] Most crude samples aren't compatible with chromatographic methods and require additional processing for further isolation and purification, such as extraction, filtration, precipitation, etc.[67] The goal of sample preparation is to obtain a representative analyte that is relatively free of interferences and maximizes the accuracy and precision of the measurement.

2.5.5 Method optimization

The actual method optimization depends on predetermined requirements such as selectivity, speed, etc. It is desirable to approach the optimization of the method systematically. The most frequently optimized parameters include flow and composition of mobile phase, temperature, and injected volume of sample. All of these parameters are optimized to maximize response, resolution and avoid peak distortions such as fronting or tailing.[67]

2.6 COSMO-RS

COSMO-RS (Conductor-like Screening Model for Real Solvents) is a computational technique designed to predict the thermodynamic properties of compounds in the liquid phase.[75] This method employs quantum mechanical calculations to predict the chemical potential of given compound, which allows prediction of other physicochemical properties (such as partition coefficients and the resulting log *P*).[76,77,78] In the first step, a quantum mechanical simulation is conducted with the molecule placed in a cavity surrounded by an ideal conductor environment, enabling the creation of a polarized surface. This leads to the distribution of polarization charge on the molecular surface, which is then analyzed in the form of a sigma-profile. The sigma-

profile illustrates the charge density distribution on the molecule's surface. This profile is utilized as input for thermodynamic calculations. In the next step, the sigma profile is used to calculate the interactions between molecules in a mixture. Based on this data, the method predicts the chemical potentials.[76,79] The advantage of the COSMO-RS method is its wide applicability and accuracy. In addition, it is able to provide insight into systems that are difficult to study experimentally, for example due to toxicity of substances.[44,80]

3. Objectives of the Thesis

1. Determination of the lipophilicity (log *P*) for a total of 11 compounds – a complete series of deoxyfluorinated analogues of methyl β-D-galactoside and methyl β-D-lactoside using the reference stir flask method with ^{19}F NMR detection.

2. Development and optimization of an alternative method for log *P* determination using hydrophilic interaction chromatography (HILIC).

3. Prediction of log *P* values using the COSMO-RS method and comparison of this values with measured log *P*.

4. Evaluation of the relationship between lipophilicity and the position of a fluorine substituent.

4. Experimental part

4.1 Structures of Investigated Compounds

In this master's thesis, the lipophilicity of deoxyfluorinated methyl β-D-galactoside and methyl β-D-lactoside (Lac) analogs was initially determined by an established method using ^{19}F NMR spectroscopy. These results in combination with the already published data of the deoxyfluorinated methyl *N*-acetyl-β-D-lactosaminide (LacNAc) series[81] were compared with the results obtained from the new HILIC-ESI-MS method. The general structure of saccharide scaffolds investigated in this study is depicted in *figures 3–5* with the appropriate carbon numbering.

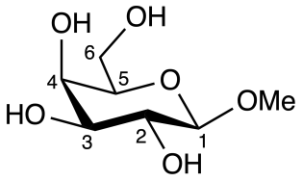

Figure 3: Methyl β-D-galactopyranoside

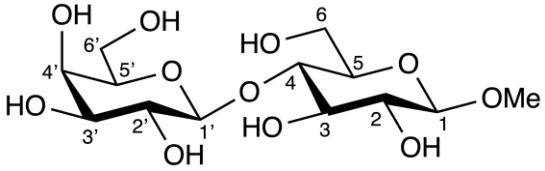

Figure 4: Methyl β-D-lactoside

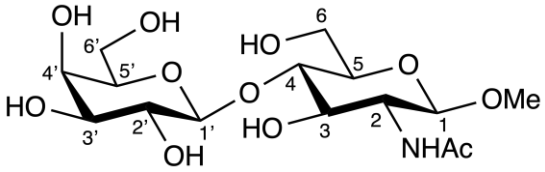

Figure 5: Methyl *N*-acetyl-β-D-lactosaminide

These samples are white crystalline compounds prepared in the Research Group of Bioorganic Chemistry and Biochemistry at the Institute of Chemical Process Fundamentals of the CAS.

4.2 General Procedures

Commercially available chemicals were purchased from available suppliers and used without further purification. The solutions were concentrated under reduced pressure at temperatures below 45 °C. Demineralized water was obtained from RO TFM-5SV reverse osmosis system. TLC chromatography was performed on silica gel 60 F254 (Sigma-Aldrich), and spots were detected with an UV lamp (254 nm) or anisaldehyde solution (EtOH/AcOH/H_2SO_4). For column chromatography, silica gel 60 (70–230 mesh, Material Harvest) was used. NMR spectra were measured on Bruker Avance III HD 400 (^{1}H at 400.1 MHz, ^{19}F at 376.4 MHz, ^{13}C at 100.6 MHz) and/or JEOL ECZ500R (^{1}H at 500.2 MHz, ^{19}F at 470.6 MHz) spectrometers at 25 °C. ^{1}H and ^{13}C NMR spectra were referenced to the residual signal of deuterated solvent ($CDCl_3$ δ_H/δ_C: 7.26 ppm/77.16 ppm, MeOH-d_4 δ_H/δ_C: 3.31 ppm/49.0 ppm). ^{19}F NMR spectra were referenced to the line of an internal standard hexafluorobenzene (−163.00 ppm in $CDCl_3$, −166.62 ppm in MeOH-d_4). The NMR data were processed by the software MestReNova. HRMS analyses were done using Bruker MicrOTOF-QIII, ESI ionization in positive or negative mode. HILIC analyses were done using Liquid chromatograf Dionex Ultimate 3000 (ThermoScientific) either with HRMS detection or ELSD detector (Polymer Laboratories PL-ELS 2100). Weight of analyte was determined by analytical balance Denver TB-215D dual range. For adjustment of pH the inoLab® Multi 9620 IDS pH meter was used.

4.3 Synthetic Procedures

The majority of investigated compounds were prepared previously in the Research Group of Bioorganic Chemistry and Biochemistry. A small portion of this master's thesis involved synthesizing some of these compounds, following established procedures.[81] Although this synthesis is not a critical aspect of this work, three reactions are noteworthy. First reaction worth mentioning is when compound **1** was obtained as a pure alpha anomer through recrystallization. Acetate **1** was prepared according to a published procedure.[81] The acetate **1** was converted into 2,4,6-tri-*O*-acetyl-3-deoxy-3-fluoro-α-D-galactopyranosyl bromide, which was used in glycosylation of methanol to provide methyl 2,4,6-tri-*O*-acetyl-3-deoxy-3-fluoro-β-D-galactoside (**2**).[82] Deacetylation of **2** subsequently provided final product methyl 3-deoxy-3-fluoro-β-D-galactoside (**3**).

1,2,4,6-Tetra-*O*-acetyl-3-deoxy-3-fluoro-D-galactopyranoside (1)

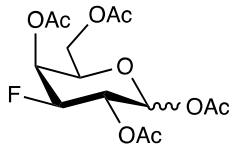

The starting compound (1,6-anhydro-3-deoxy-3-fluoro-β-D-galactopyranoside; 600 mg, 3.66 mmol)[81] was dissolved in 18 mL of acetic anhydride. The reaction mixture was cooled down to 0 °C and TESOTf (56 μl, 0.25 mmol) was added. The reaction mixture was stirred for one hour at 0 °C and overnight at room temperature. TLC (EtOAc/PE 1:1) showed complete consumption of the starting material. The reaction mixture was diluted with EtOAc and poured onto ice. Saturated aqueous solution of $NaHCO_3$, and solid $NaHCO_3$ were added, and the reaction mixture was stirred for approximately 2 hours until the gas evolution ceased. Phases were separated and the water phase was extracted with EtOAc three times. Organic phases were combined, dried with anhydrous Na_2SO_4, and concentrated under reduced pressure. Purification of crude products by column chromatography (EtOAc/PE 2:3) provided compound **1** (1.15 g, 90%) as yellowish solid. The product was then recrystallized from ethanol providing α-anomer as a white crystalline solid. NMR data were in accordance with the published data.[81] Data for **1**: mp 130–133 °C (ethanol), HRMS (ESI-MS) *m/z*: $[M + Na]^+$ calculated for $C_{14}H_{19}FO_9$: 373.0911, measured: 373.0905 , $[\alpha]_D^{20}$ +131 (*c* 0.265 g/100mL, $CHCl_3$).

Methyl 2,4,6-tri-*O*-acetyl-3-deoxy-3-fluoro-D-galactopyranoside (2)

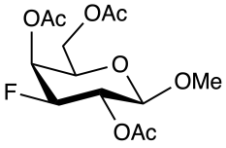

2,4,6-Tri-*O*-acetyl-3-deoxy-3-fluoro-α-D-galactopyranosyl bromide (250 mg, 0.67 mmol) was prepared from compound **1** using a reported procedure.[81] This bromide was dissolved in 4 mL of MeOH and molecular sieves were added. The reaction mixture was cooled down to 0 °C and iodine (100 mg, 0.39 mmol) was added under the argon atmosphere. The reaction mixture was stirred for 3 hours at room temperature and saturated aqueous solution of $Na_2S_2O_7$ was added afterwards. The suspension was filtered, and the filtrate was extracted with EtOAc three times. Organic phases were combined and washed with saturated aqueous $NaHCO_3$. The mixture was concentrated under reduced pressure. Purification of crude product by column chromatography (EtOAc/PE 1:1) provided compound **2** (192 mg, 88%) as off-white crystalline solid. NMR data were in accordance with already published data.[83]

Methyl 3-deoxy-3-fluoro-β-D-galactopyranoside (3)

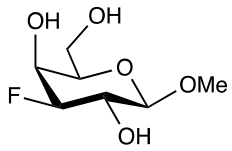

The starting compound (methyl 2,4,6-tri-*O*-acetyl-3-deoxy-3-fluoro-β-D-galactopyranoside, 140 mg, 0.47 mmol) was dissolved in 2 mL of MeOH. With constant stirring, a solution of 0.5 M NaOMe in MeOH was added dropwise until pH ~ 9, and the reaction mixture was stirred for 1 hour at room temperature. TLC (EtOAc/PE 1:1) showed complete consumption of the starting material. DOWEX 50W ion exchange resin was added to the reaction mixture until the pH was neutral. The suspension was filtered and the filtrate was concentrated under reduced pressure.[81] Product was recrystallized from methanol providing white crystalline solid (90 mg, 98%). Data for **3**: mp 165–167 °C (methanol), ^{1}H NMR (400 MHz, Methanol-d_4, ^{1}H{^{19}F}, H−H COSY, HSQC) δ 4.35 (ddd, 1H, J = 48.7, 9.5, 3.5 Hz, H-3), 4.15 (d, 1H, J = 7.7 Hz, H-1), 4.07 (dd, 1H, J = 6.6, 3.5 Hz, H-4), 3.82 – 3.70 (m, 3H, H-2, H-6), 3.57 – 3.45 (m, 4H, H-5, CH_3). ^{13}C NMR (101 MHz, Methanol-d_4, HSQC) δ 103.94 (d, J = 12.0 Hz, C-1), 93.57 (d, J = 185.1 Hz, C-3), 73.95 (d, J = 6.9 Hz, C-5), 69.53 (d, J = 18.6 Hz, C-2), 66.93 (d, J = 16.8 Hz, C-4), 60.66 (d, J = 3.3 Hz, C-6), 56.01 (CH_3). ^{19}F NMR (376 MHz, Methanol-d_4) δ −200.81 (ddd, J = 48.7, 13.0, 6.5 Hz). HRMS (ESI-MS) *m/z*: $[M + Na]^+$ calculated for $C_7H_{13}FO_5$: 219.0645, measured: 219.0639, $[\alpha]_D^{20}$ −20 (c 0.255 g/100mL, $CHCl_3$).

4.4 Determination of Lipophilicity by Stir-flask Method with ^{19}F NMR Detection

Lipophilicity was determined by the direct method of thermodynamic partition of the investigated substance between water and n-octanol. This method, recently published by Linclau, utilizes the relative integral intensity signal from fluorine in ^{19}F NMR in octanol and water phases. This method relies on comparing the relative integral intensities of the examined substance and a standard with known log P in both phases.[1]

4.4.1 Sample Preparation

The tested fluorinated saccharide (6 – 15 mg) and reference compound with known lipophilicity (2-fluoroethanol, ~ 0.2 μL) were dissolved in demineralized water (1 – 1.5 mL) in a 10 mL pear-shaped flask and the same volume of n-octanol was added. The resulting emulsion was vigorously stirred for a minimum of 3 hours at 25 °C and then left to stand overnight at 25 °C. The biphasic system was carefully transferred into a 2 mL vial and centrifuged at 6000 rpm for

20 minutes, ensuring optimal separation of phases. The 0.5 mL of octanol phase was carefully withdrawn using a 1 mL disposable syringe. After wiping the needle dry, the octanol phase was slowly injected into an NMR tube. Another disposable syringe was used to collect 0.6 mL of the water phase. To prevent contamination of the water sample by the octanol phase, 0.1 mL of air was taken into the syringe before inserting the needle into the biphasic system. Some of the air in the syringe was pushed out as it passed through the upper octanol phase. As the needle entered the water phase, the remaining air was expelled, and the 0.6 mL water phase was carefully collected. The needle was wiped dry, and 0.1 mL of the solution was discarded to prevent cross-contamination by the octanol phase. The remaining 0.5 mL was injected into a second NMR tube. Both NMR tubes were visually inspected to ensure that there was no apparent contamination of one phase by the other, and then aceton-d_6 (0.1 mL) was added to both NMR tubes. NMR tubes were sealed by a blow torch and homogenized using VORTEX homogenizer.

4.4.2 NMR experiments

For lipophilicity determination, $^{19}F\{^{1}H\}$ spectra were measured using Bruker Avance III HD 400 and JEOL ECZ500R spectrometers. The point of transmitter frequency offset was adjusted to be in the middle of the two ^{19}F signals. The number of transients was carefully chosen to maintain an adequate signal-to-noise ratio for diagnostic signals in both phases (NS for water phase 8–32, NS for octanol phase 256–13 000). Depending on the tested compound, the width of the spectral window was selected to visualize all diagnostic signals (100 ppm). The interscan relaxation delay was set to 30 seconds in the water phase and 15 seconds in the octanol phase.[81] The NMR data were processed by the MestReNova program using the following parameters: Exponential apodization (2.00 Hz) and Zero Filling 265144 (256K) followed by manual phase correction and multipoint baseline correction.

4.4.3 Calculation of Log *P*

The lipophilicity of fluorinated saccharides was described with log *P* values, determined from relative integrals of ^{19}F signals in NMR spectra. The signal of the fluorinated standard was integrated, and the relative value of the integral was set to 100.000. Then the signal of the measured saccharide was integrated, and the log *P* value was calculated using the following formulas.[1]

$$\rho_W = \frac{I_W^X}{I_W^S} \tag{9}$$

ρ_W – the ratio of the relative integral of the tested saccharide (X) and the fluorinated standard (S) in the water phase

I_W^X – Relative integral of the tested saccharide (X) in the water phase

I_W^S – Relative integral of the standard (S) in the water phase

$$\rho_O = \frac{I_O^X}{I_O^S} \tag{10}$$

ρ_O – the ratio of the relative integral of the tested saccharide (X) and the fluorinated standard (S) in the octanol phase

I_O^X – Relative integral of the tested saccharide (X) in the octanol phase

I_O^S – Relative integral of the standard (S) in the octanol phase

$$\log P^X = \log P^S + \log\left(\frac{\rho_O}{\rho_W}\right) \tag{11}$$

P^X – octanol/water partition coefficient of tested saccharide

P^S – octanol/water partition coefficient of fluorinated standard ($\log P^S = -0.75$)[81]

4.5 Determination of lipophilicity using HILIC

During the development of the HILIC method, two types of detectors were used: ELSD and ESI-MS. During the optimization of the method, the ELSD detector was employed; however, it proved to be impractical and insufficiently sensitive. For these reasons, it was replaced by the ESI-MS detector, which turned out to be more suitable for the intended purposes.

4.5.1 Sample preparation

The samples for the determination of lipophilicity by HILIC-ESI-MS method were prepared as follows. Deoxyfluorinated saccharide (0.5 mg) was dissolved in a mixture of ACN and demineralized water (1:1, 1 mL). The samples were then diluted with the same mixture of ACN and demineralized water (1:1) to a concentration of 0.025 mg/mL (1 mL), and a standard compound, methyl β-D-glucopyranoside (10 μL, 2.5 mg/mL), was added to the 1.5 mL vial.

Samples for optimization of method using HILIC-ELSD we prepared analogously. Deoxyfluorinated saccharide (0.5 mg) was dissolved in a mixture of ACN and demineralized water (1:1, 1 mL). The samples were then diluted with the same mixture of ACN and demineralized water (1:1) to a concentration of 0.25 mg/mL (1 mL), and a standard compound, D-glucose (10 μL, 25 mg/mL), was added to the 1.5 mL vial.

4.5.2 Mobile phase preparation

The mobile phase consisted of a mixture of ACN and ammonium acetate buffer (10 mM, pH 6.4). For each measurement, the ammonium acetate buffer was freshly prepared by weighing 192.7 mg of ammonium acetate and dissolving it in about 200 mL of demineralized water. The pH of the mixture was then adjusted to 6.4 using diluted acetic acid, and the solution was brought to a final volume of 250 mL

4.5.3 Method optimization

Method optimization was performed on the deoxyfluorinated methyl *N*-acetyl-β-D-lactosaminide (LacNAc) series using ELSD detection. In my hands, the ELSD detection method was identified as highly unreliable, suffering from low sensitivity and disastrous reproducibility. The signals of the injected compounds gradually weakened or even

disappeared, so that the detection of any compound became impossible after 10 injections. I suggest that this observation is due to fouling of the ELSD detector by the use of ammonium acetate buffer. Although the function and sensitivity of the ELSD detector could have been restored by a steam cleaning procedure, this would have had to be repeated on a frequent basis, which was considered to be highly impractical. For these reasons, the ELSD detector was replaced by a more sensitive ESI-MS detector. In contrast to the optimized measurement, a different standard – D-glucose - was used in the optimization procedure of the mobile phase. It turned out to be less suitable due to its retention time when there was an overlap of signals with one of the samples. Methyl β-D-glucopyranoside had a shorter retention time than all samples, making it a suitable standard. After conducting a literature review, a series of tests was performed with 3F-LacNAc compound, that had the lowest log *P* of the entire series.[81] Various mobile phase ratios, sample volumes and sample concentrations were tested. Before every measurement, the column was conditioned with ACN/ammonium acetate buffer (10 mM, pH 6.4) 50:50 for 30 minutes and then washed for 1 hour with the chosen mobile phase. After the measurement, the column was washed for half an hour with a mixture of ACN/H_2O 80:20, in which the column was stored.

4.5.4 Statistical processing

After determining the optimal conditions, three measurements were performed with each sample to determine the repeatability of the method (these measurements were made with MS detection, as already mentioned). From the results obtained, the standard deviation with Bessel's correction[84] and relative standard deviation were determined using the following formulas:

$$SD = \sqrt{\frac{\sum_{i=1}^{n}(x_i - \bar{x})^2}{n-1}} \tag{12}$$

where $\bar{x}$ is the average value of all measurements, x_i is the value of the i-th measurement, and n is the total number of measurements. The relative standard deviation can be calculated from the relationship:

$$RSD[\%] = \frac{SD}{\bar{x}} \cdot 100 \tag{13}$$

4.6 COSMO-RS Calculations

COSMO-RS calculations were performed by Ing. Martin Balouch, Ph.D. at the University of Chemistry and Technology in Prague.

The selected DFT-minimized geometries (DFT calculations were performed in Gaussian16-B.01), representing the most stable conformers of LacNAc and Lac compounds, were used to calculate log *P* using the COSMO-RS method. Each chosen conformer underwent vacuum and water optimization with a fine grid option, using Turbomole 6.3. The .cosmo files for each conformer were generated from this process and subsequently utilized for the partitioning calculations. Using the COSMOtherm X18 software and the .cosmo files of all calculated conformers, the chemical potential of the molecules in water and water-saturated octanol was computed, providing the partition coefficients.[85]

5. Results and Discussion

5.1 Results of log *P* determination by ^{19}F NMR

Lipophilicity expressed as log *P* was determined for deoxyfluorinated methyl D-galactopyranosides and deoxyfluorinated methyl β-D-lactosides using established ^{19}F NMR method.[54] Obtained results were compared with the published lipophilicities of mono-deoxyfluorinated-D-glucopyranososes[86] and mono-deoxyfluorinated methyl *N*-acetyl-β-D-lactosaminides.[81]

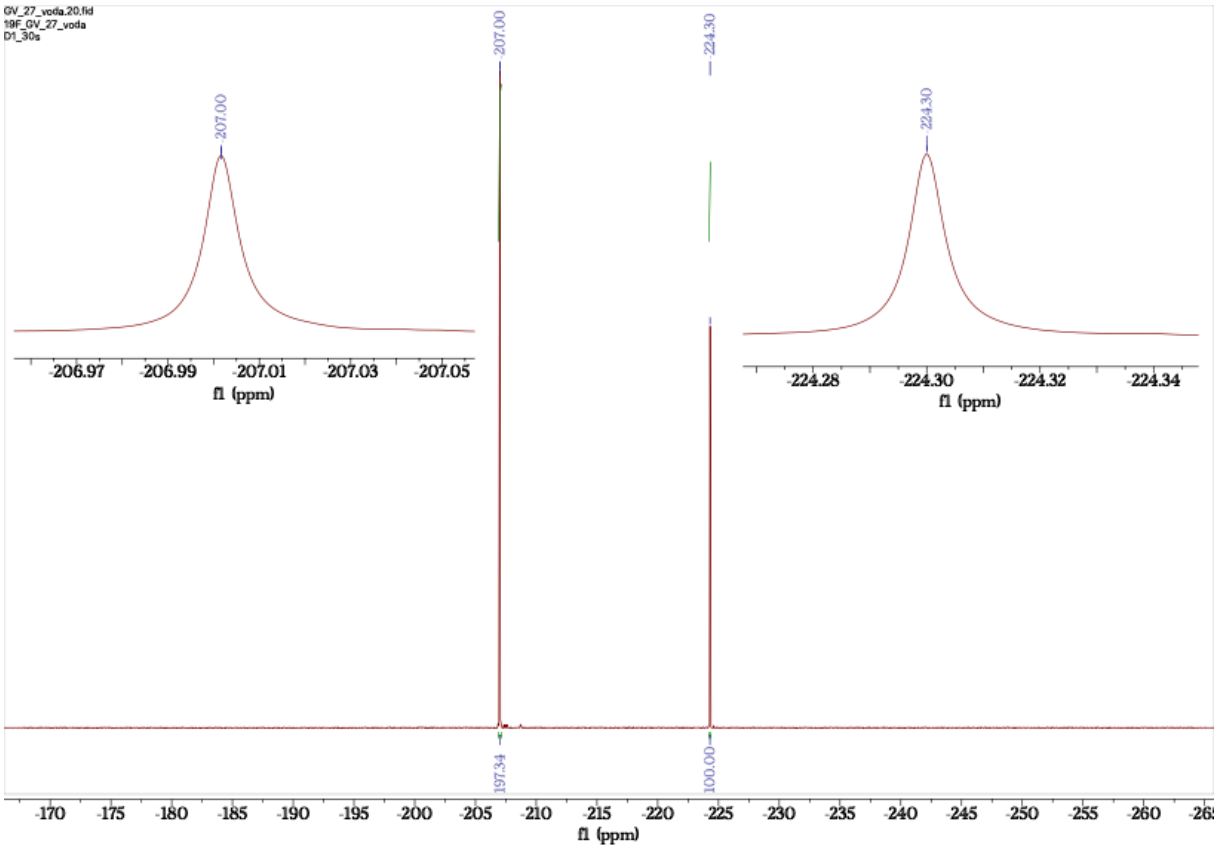

Figure 6: Example of ^{19}F{^{1}H} NMR spectra of 2′F-Lac – water phase. Spectrometer: Bruker Avance III HD 400, NS: 16, solvent: acetone-d_6, relaxation delay: 30 s

Figure 6 shows the NMR spectra of the aqueous phase and two intense peaks in it, of which the peak with a shift of −224.30 ppm belongs to the standard (2-fluoroethanol) and the peak with a shift of −207.00 ppm belongs to 2' deoxyfluorinated methyl-β-D-lactoside (2'F-Lac). Since

carbohydrates are very hydrophilic compounds, all NMR spectra of the water phase provide a good signal-to-noise ratio.

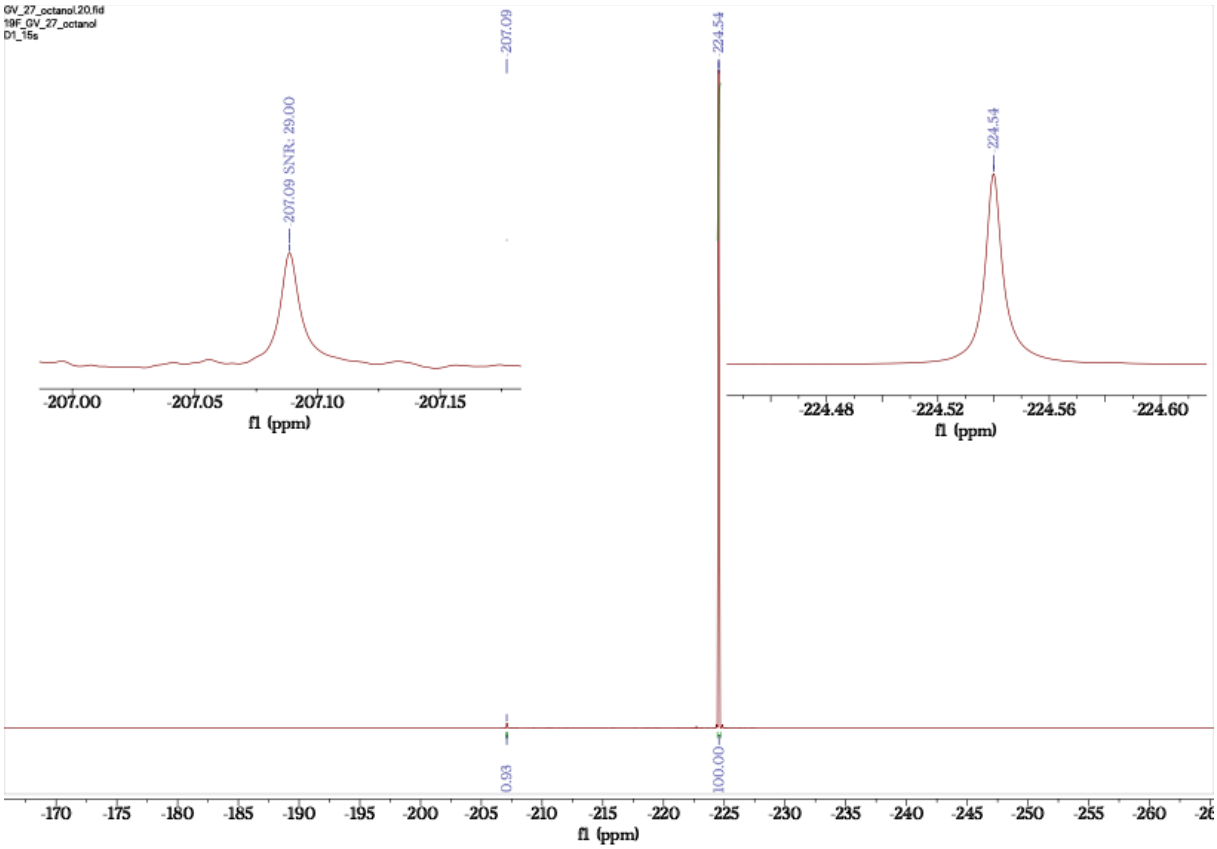

Figure 7: Example of $^{19}F\{^{1}H\}$ NMR spectra of 2′F-Lac – octanol phase. Spectrometer: Bruker Avance III HD 400, NS: 10 800, solvent: acetone-d_6, relaxation delay: 15 s

Similarly, *Figure 7* shows the NMR spectrum of the octanol phase with two peaks in it, of which the peak with a shift of −224.54 ppm belongs to the standard (2-fluoroethanol), and the peak with a shift of −207.09 ppm belongs to 2'F-Lac. The signal-to-noise ratio was established at 29.00. Even though S/N for quantitative NMR is recommended to be at least 250:1 for integration errors to be negligible (< 1%)[53], it was proven by Linclau[1], that for very hydrophilic compounds such as carbohydrates, reliable integration ratios can be still obtained with S/N ratio lower than 100:1. Linclau illustrates with three examples, that the integration ratios for the number of scans NS 64 and NS 4096 are almost identical, which leads to nearly identical log *P* values, even for S/N 21. Signal to noise ratio higher than 21 was achieved in all measurements

by optimizing the number of scans and/or by using more sensitive high-field 500 MHz NMR JEOL NMR spectrometer.

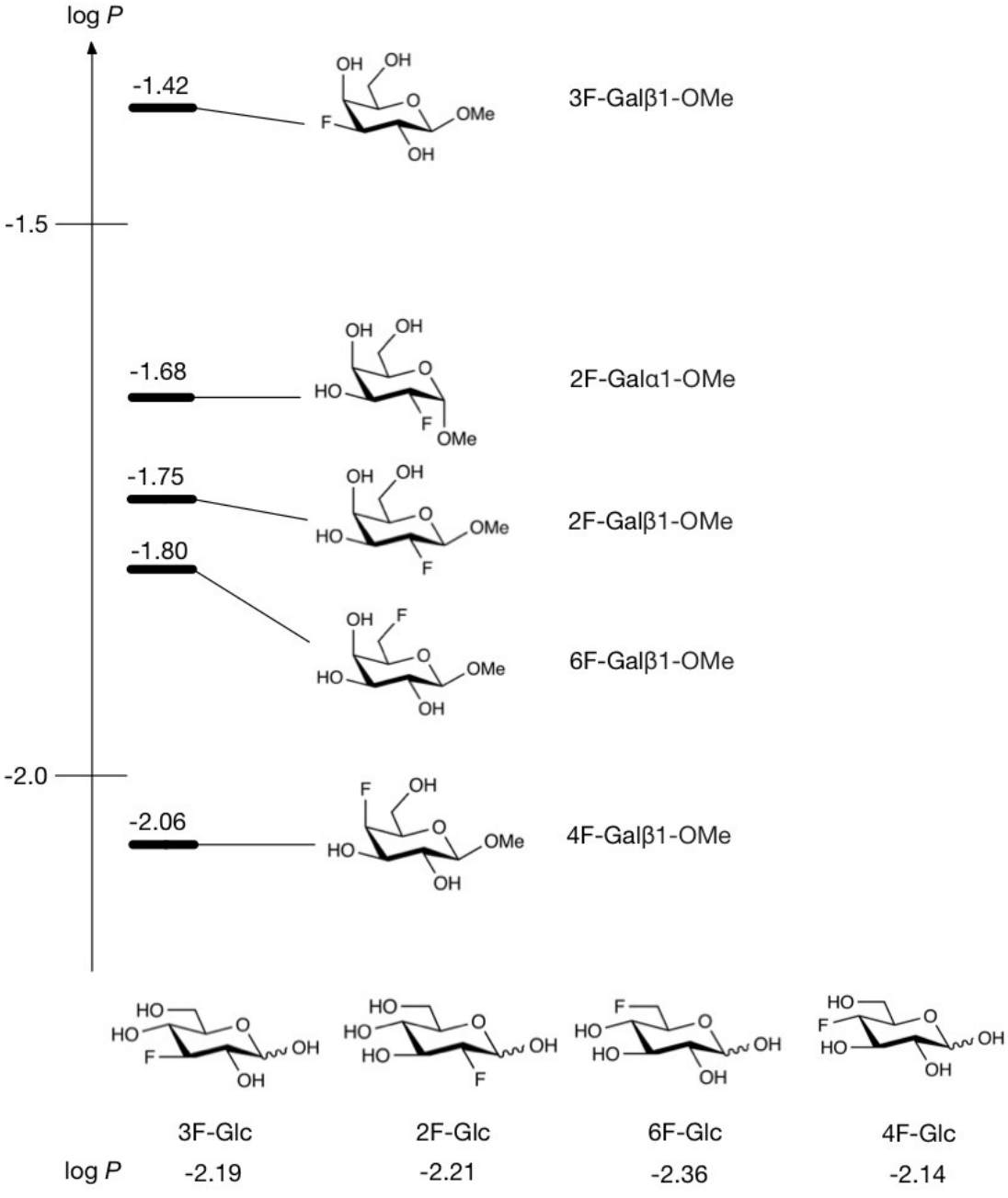

Figure 8: log *P* values of mono-deoxyfluorinated methyl β-D-galactopyranosides and deoxyfluorinated D-glucopyranosides (Glc) calculated from $^{19}F\{^{1}H\}$ NMR spectra. Methyl 2-deoxy-2-fluoro-D-galactopyranoside (2F-Gal-OMe) was obtained as a mixture of α and β anomers apparent in ^{19}F NMR spectra.

Log *P* values of monodeoxyfluorinated methyl β-D-galactopyranosides (Galβ1-OMe) were in a range from −2.06 to −1.42. 3F-Galβ1-OMe showed the highest lipophilicity (log *P* = −1.42). The substances 2F-Galα1-OMe, 2F-Galβ1-OMe, 6F-Galβ1-OMe had very similar lipophilicities in the interval from −1.80 to −1.68. 4F-Galβ1-OMe showed the lowest lipophilicity of the galactopyranoside series (log *P* = −2.06). Comparison with recently reported data for deoxyfluorinated D-glucopyranoses[86] (Glc, *Figure 8*) revealed that Log *P* values of deoxyfluorinated Galβ1-OMe analogs were generally higher. This result was expected, as the monodeoxyfluorinated D-glucopyranoses have four free hydroxyl groups in structures whereas mono deoxyfluorinated Galβ1-OMe analogs have only three free hydroxyls. Series of Galβ1-OMe analogs also showed more significant differences in log *P* values in individual compounds (max. Δlog *P* = 0.64) than D-glucopyranoses (max. Δlog *P* = 0.22) emphasizing the complex influence of saccharide configuration on its lipophilicity.

Completely different results in lipophilicity were observed between 4F-Glc and 4F-Galβ1-OMe. Whereas 4F-Glc was identified as the least hydrophilic in the series of D-glucopyranoses, 4F-Galβ1-OMe was the most hydrophilic compound in the series of Galβ1-OMe. This difference likely arises from the configuration at position C4. In 4F-Glc, the fluorine is in an equatorial position, whereas in 4F-Galβ1-OMe it is oriented axially. Apart from that, the increasing trend of log *P* remains consistent with the order 3F > 2F > 6F for both Glc and Galβ1-OMe series.

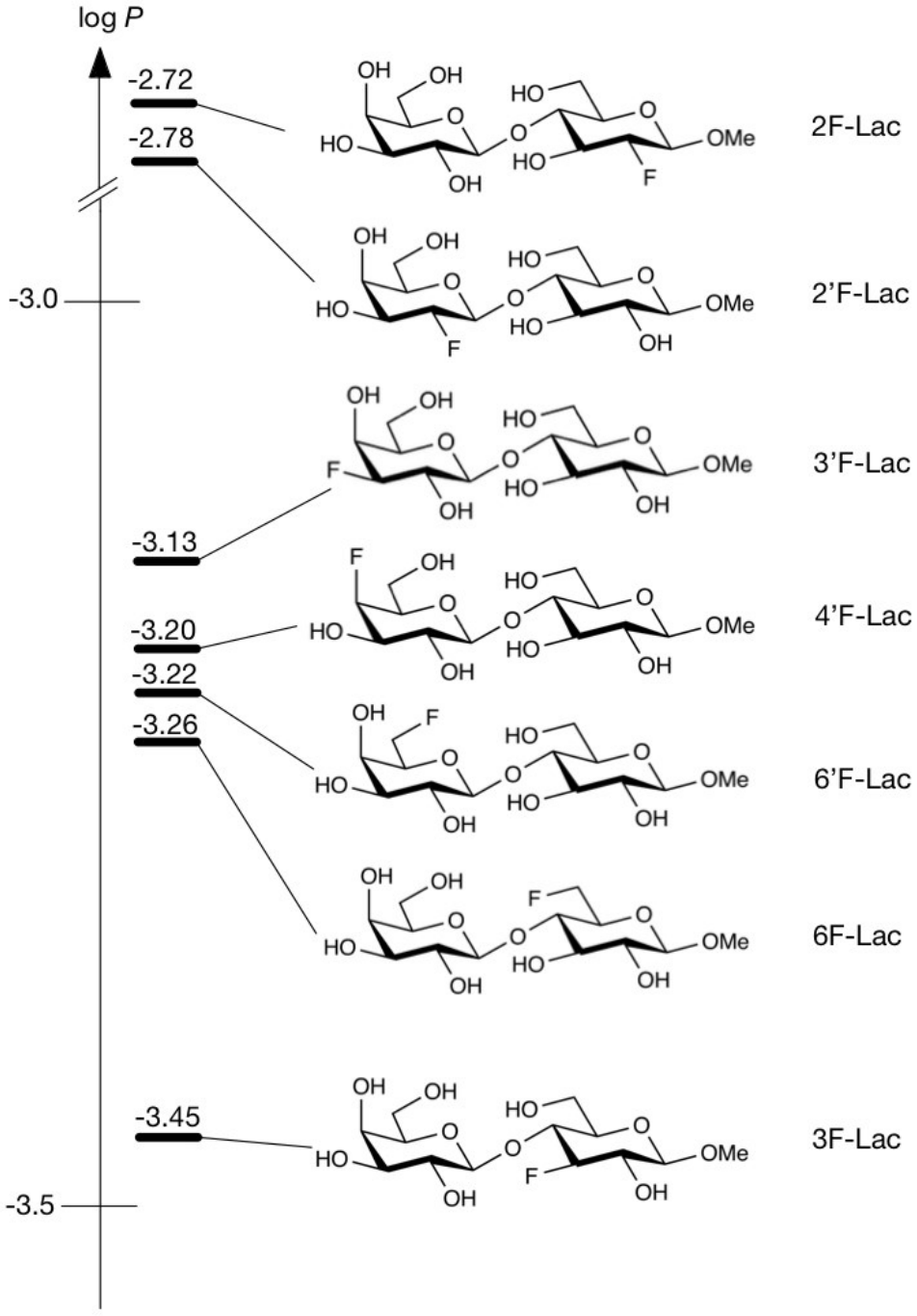

Figure 9: log *P* values of deoxyfluorinated methyl β-D-lactosides (Lac) calculated from $^{19}F\{^{1}H\}$ NMR spectra.

Log *P* values of deoxyfluorinated methyl β-D-lactosides were in range from −3.45 to −2.72. Compared to the D-glucose and methyl D-galactoside series, lipophilicities of deoxyfluorinated lactosides are lower with a more significant deviations between individual compounds (max.

Δlog *P* = 0.73). 3F-Lac showed the lowest lipophilicity (log *P* = −3.45). The substances 6F-Lac, 6′F-Lac, 4′F-Lac and 3′F-Lac showed very similar lipophilicities in the interval from −3.26 to −3.13. Fluorination to the C2 and C2′ positions gave compounds with the highest lipophilicity in Lac series with log *P* = −2.78 for 2′F-Lac and log *P* = −2.72 for 2F-Lac.

These results are in good agreement with previously reported log *P* values of deoxyfluorinated methyl *N*-acetyl-β-D-lactosaminides (LacNAc) shown in *Figure 11*.[81] Similarly to the series of D-lactosides, deoxyfluorination at the C2′ position in the LacNAc scaffold resulted in a compound with highest lipophilicity. Conversely, deoxyfluorination at the C3 position provided compounds with the lowest log *P* values in both series investigated (Lac and LacNAc). A hypothesis for this phenomenon was proposed and demonstrated by my colleagues on the LacNAc series. To explain the low relative lipophilicity of 3F-LacNAc, the following hypothesis has been proposed: In β1→4 linked oligosaccharides composed of pyranose units, the presence of the hydrogen bond $O5\cdots H-O3$ was previously demonstrated (*Figure 10)*.[85] Since hydroxyl OH-3 is involved in a hydrogen bond, it cannot be fully solvated. Therefore, deoxyfluorination at the C3 position does not increase lipophilicity to the same extent as deoxyfluorination at other positions.[85]

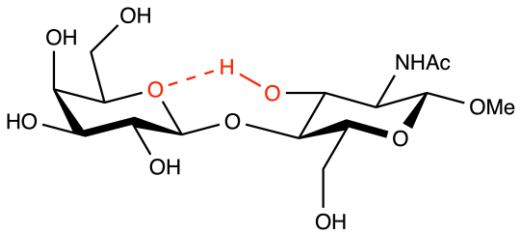

Figure 10: $O5\cdots H-O3$ hydrogen bond in methyl *N*-acetyl-β-D-lactosaminide

In all series, there is quite a large difference between the lipophilicity of the least hydrophilic compound and the most hydrophilic compound. These differences are caused only by the change in the position of the fluorine substituent.

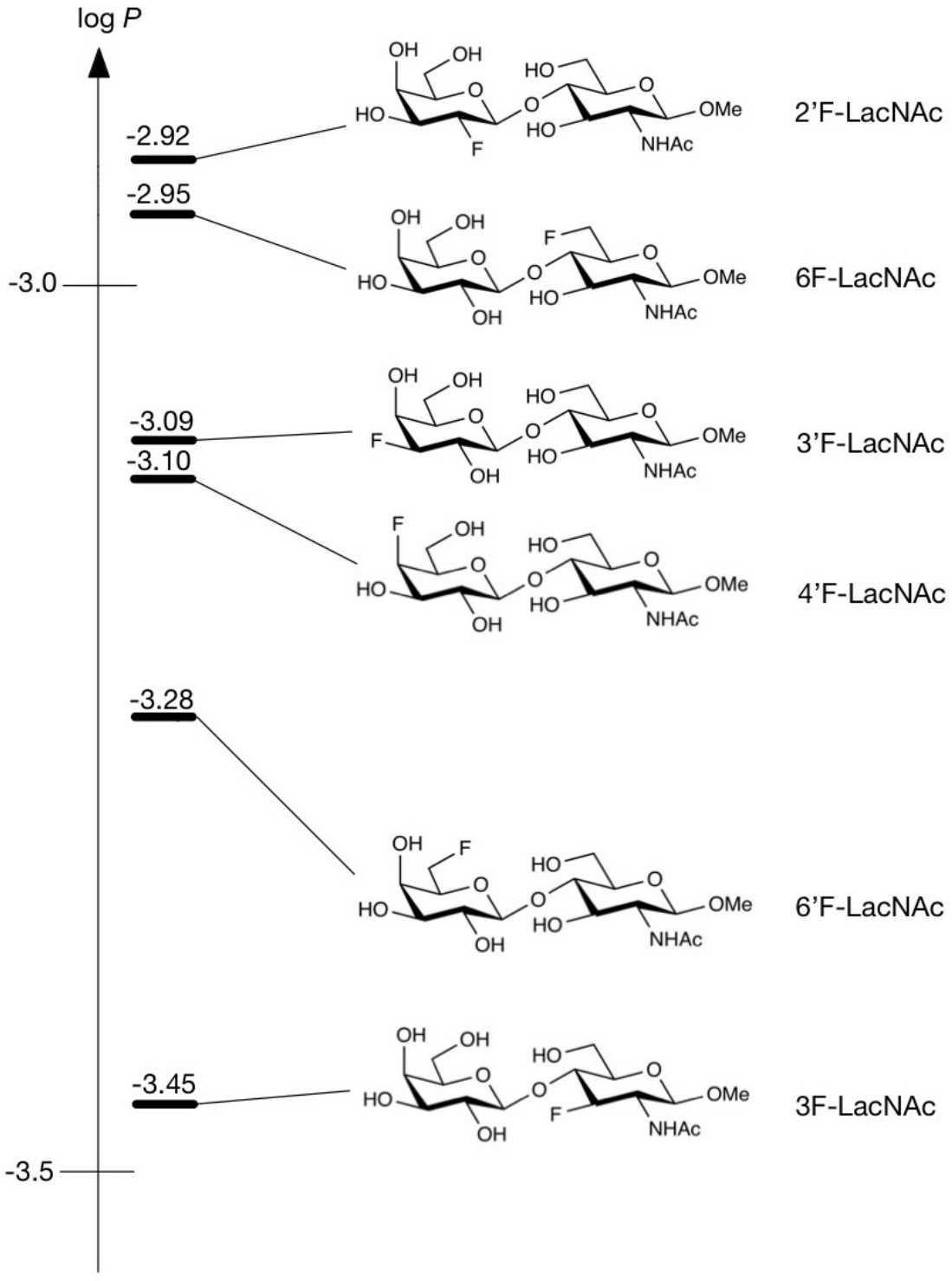

Figure 11: Previously reported log *P* values of deoxyfluorinated *N*-acetyl-β-D-lactosaminides.[81]

5.2 Results of HILIC-MS determination

5.2.1 Method optimization

Method optimization was performed on the deoxyfluorinated methyl *N*-acetyl-β-D-lactosaminide (LacNAc) series using ELSD detection.

The constant measurement conditions were set as follows:

Column: Luna Omega 3 µm Sugar 100 Å, 150 × 2.1 mm

mobile phase flow: 0.3 mL/min

Conditions for ELSD detector:

evaporation temperature: 90 °C

nebulization temperature: 50 °C

nitrogen flow: 1.6 SLM

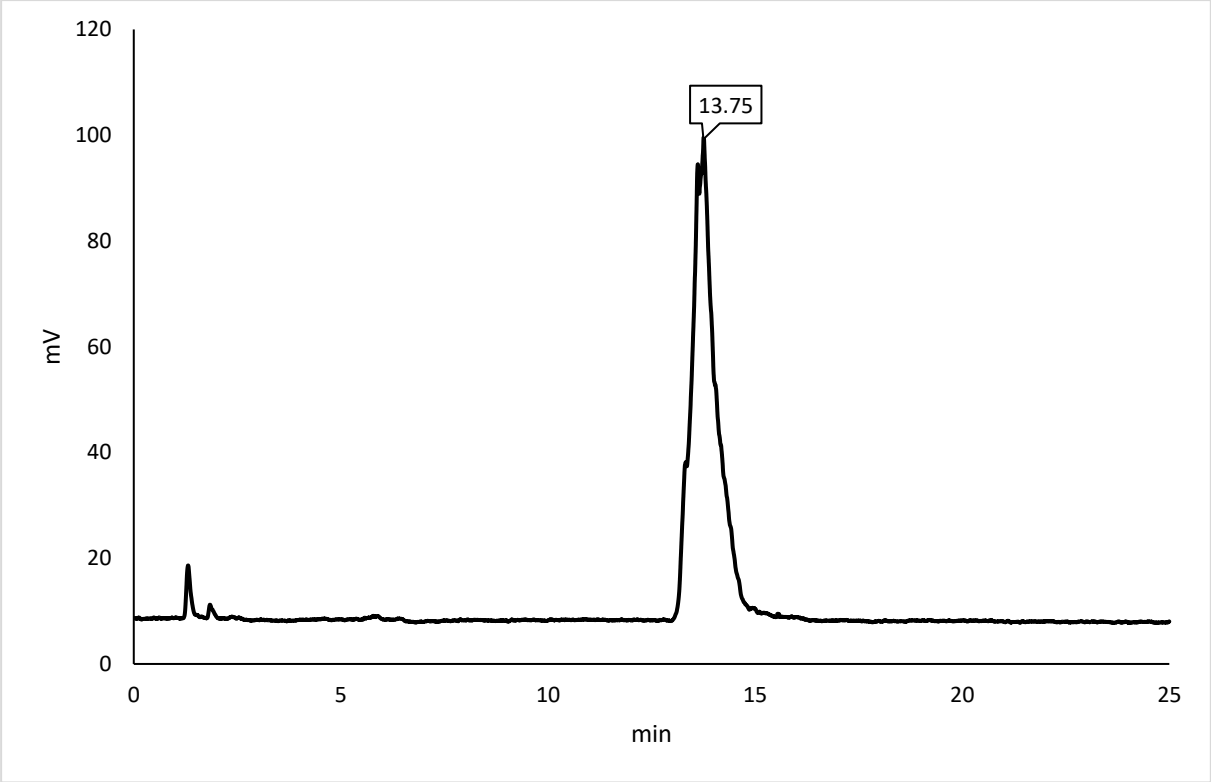

Figure 12: 3F-LacNAc chromatogram - ACN/ammonium acetate buffer (10 mM, pH 6.4) 90:10, sample concentration: 0.5 mg/mL, injection volume: 5 μL, mobile phase flow: 0.3 mL/min, column: Luna Omega 3 μm Sugar 100 Å (150 × 2.1 mm), column temperature: 25 °C, detector: ELSD

First tests on the column were performed on 3F-LacNAc (*Figure 12*). For mobile phase 90 % ACN the retention time of the sample was 13.75 minutes. Under these conditions the peak showed abnormalities – splitting.

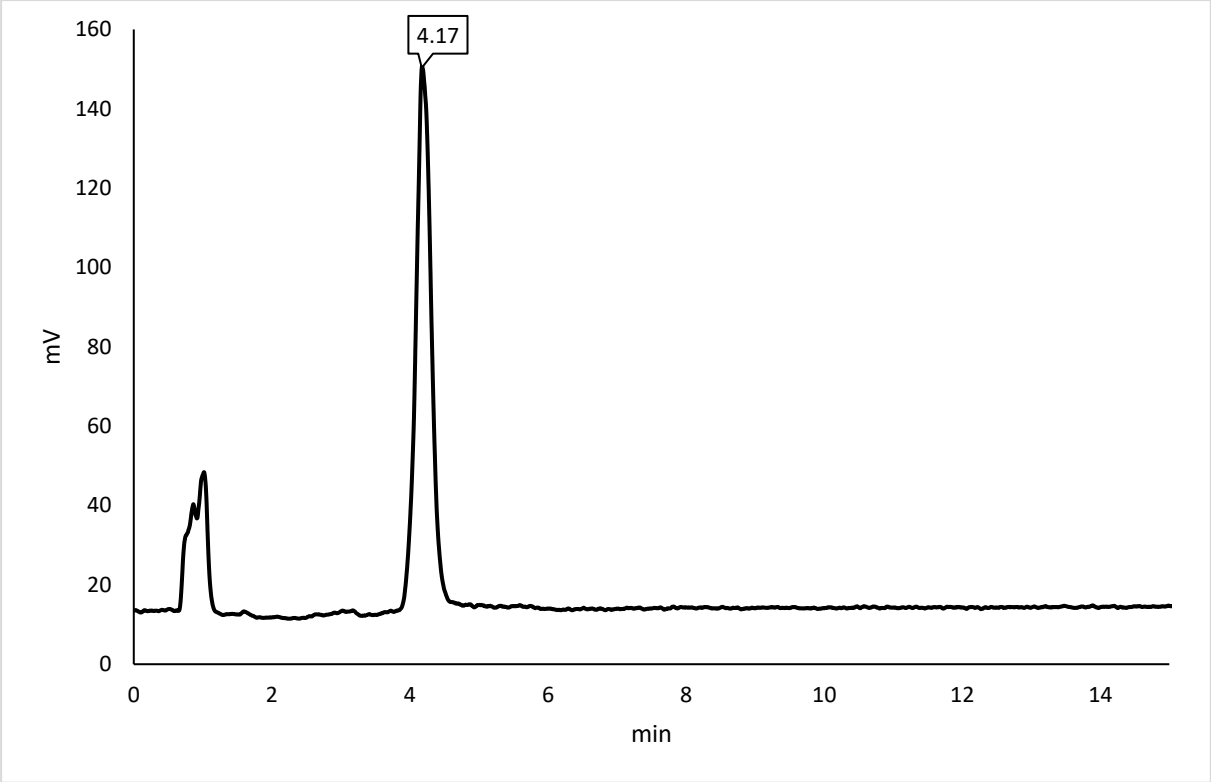

Figure 13: 3F-LacNAc chromatogram - ACN/ammonium acetate buffer (10 mM, pH 6.4) 80:20, sample concentration: 0.5 mg/mL, injection volume: 5 µL, mobile phase flow: 0.3 mL/min, column: Luna Omega 3 µm Sugar 100 Å (150 × 2.1 mm), column temperature: 25 °C, detector: ELSD

Utilizing a mobile phase ratio of ACN/ammonium acetate buffer 80:20 (*Figure 13*) significantly reduced retention time of 3F-LacNaA to 4.17 minutes. With the use of this more polar mobile phase, the peak did not show any apparent splitting.

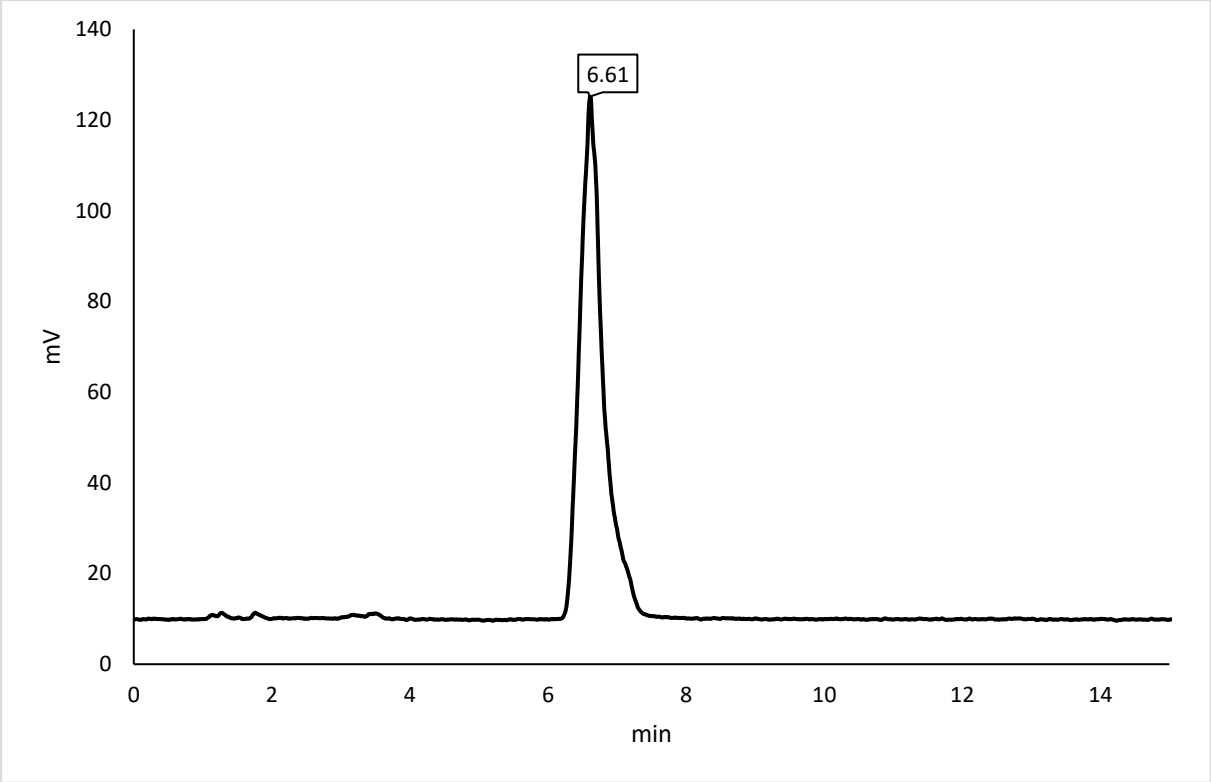

Figure 14: 3F-LacNAc chromatogram - ACN/ammonium acetate buffer (10 mM, pH 6.4) 85:15, sample concentration: 0.5 mg/mL, injection volume: 5 µL, mobile phase flow: 0.3 mL/min, column: Luna Omega 3 µm Sugar 100 Å (150 × 2.1 mm), column temperature: 25 °C, detector: ELSD

Due to the short retention time of the least lipophilic 3F-LacNAc when using a mobile phase ratio of 80:20, a mobile phase ratio of 85:15 was tested with retention time of the compound 6.61 min. Under these conditions the peak showed again some abnormalities in shape, such as tailing, as shown in *Figure 14*.

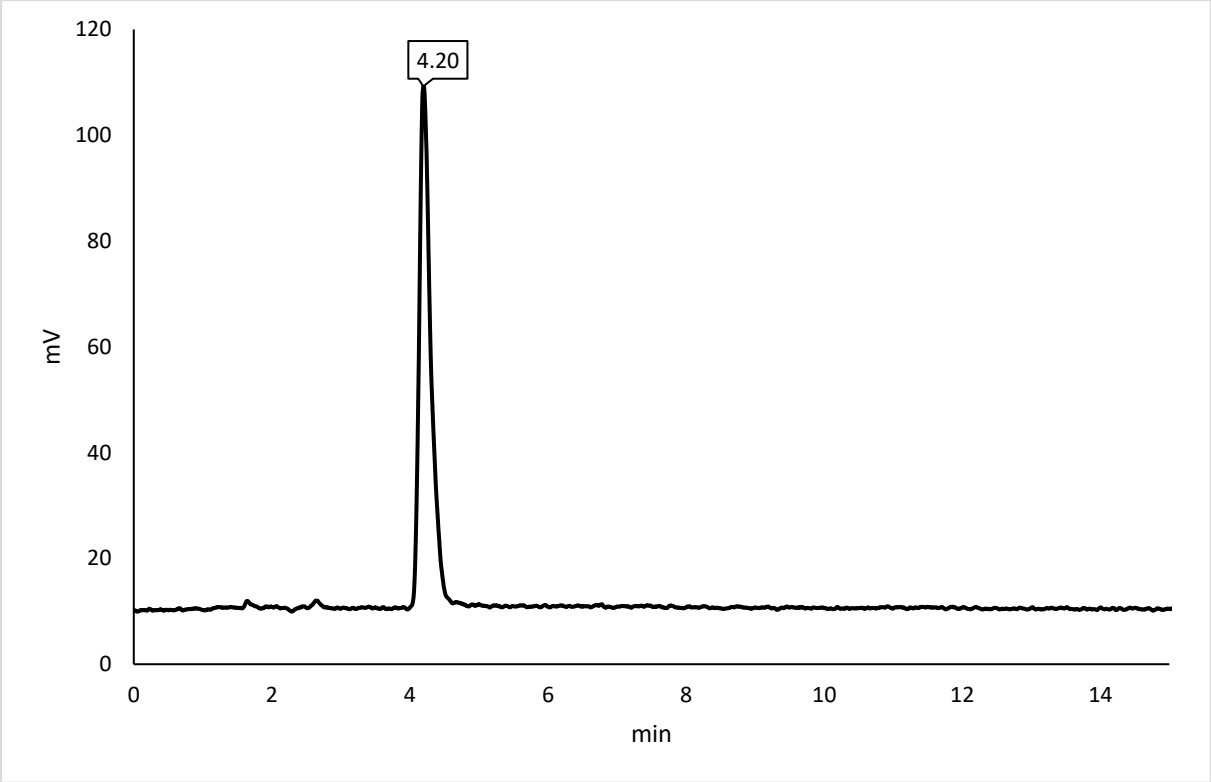

Figure 15: 3F-LacNAc chromatogram - ACN/ammonium acetate buffer (10 mM, pH 6.4) 80:20, sample concentration: 0.5 mg/mL, injection volume: 2 µL, mobile phase flow: 0.3 mL/min, column: Luna Omega 3 µm Sugar 100 Å (150 × 2.1 mm), column temperature: 25 °C, detector: ELSD

To improve the appearance of the peak, a lower injection volume (2 µL) was tested. *Figure 15* shows that for a mobile phase ratio of 80:20, the peak did not show any abnormalities, but its retention time was relatively short, which was not suitable for the given purposes.

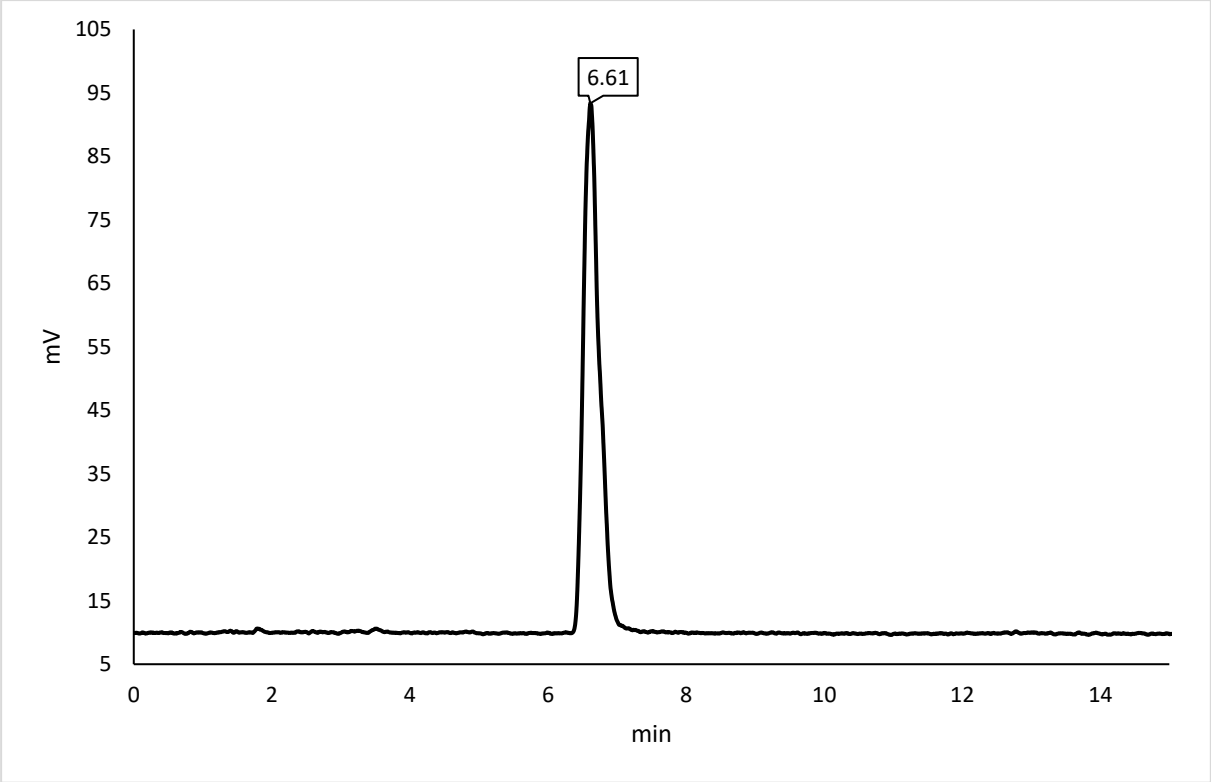

Figure 16: 3F-LacNAc chromatogram - ACN/ammonium acetate buffer (10 mM, pH 6.4) 85:15, sample concentration: 0.5 mg/mL, injection volume: 2 µL, mobile phase flow: 0.3 mL/min, column: Luna Omega 3 µm Sugar 100 Å (150 × 2.1 mm), column temperature: 25 °C, detector: ELSD

Figure 16 shows a notable improvement in peak appearance when using the same mobile phase as in the previous chromatogram (*Figure 14*). This improvement was accomplished by decreasing the injection volume from 5 µl to 2 µl.

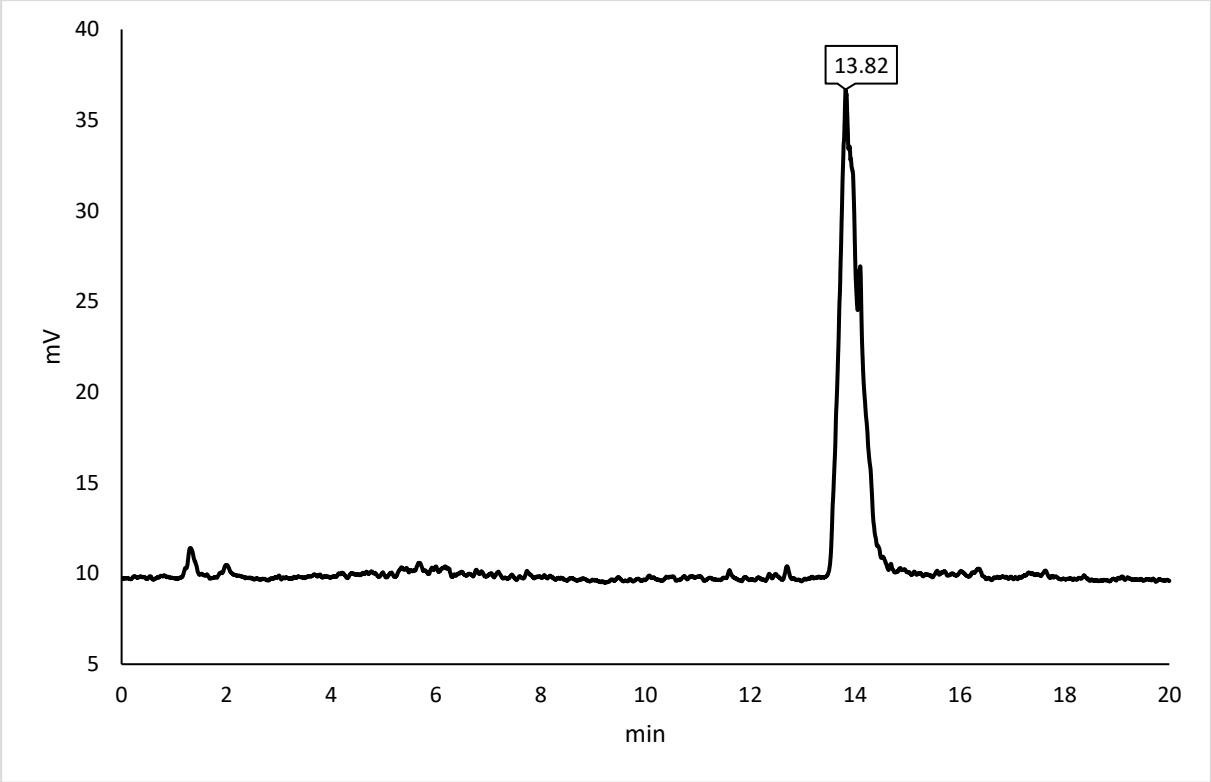

Figure 17: 3F-LacNAc chromatogram - ACN/ammonium acetate buffer (10 mM, pH 6.4) 90:10, sample concentration: 0.5 mg/mL, injection volume: 2 µL, mobile phase flow: 0.3 mL/min, column: Luna Omega 3 µm Sugar 100 Å (150 × 2.1 mm), column temperature: 25 °C, detector: ELSD

Since a significant improvement in peak shape was observed when the injection volume was reduced from 5 µL to 2 µL, this strategy was tested for the 90:10 mobile phase ratio (*Figure 17*). This adjustment provided better peak shape compared to the *Figure 12*, but still showed noticeable splitting and deviation from the gaussian shape.

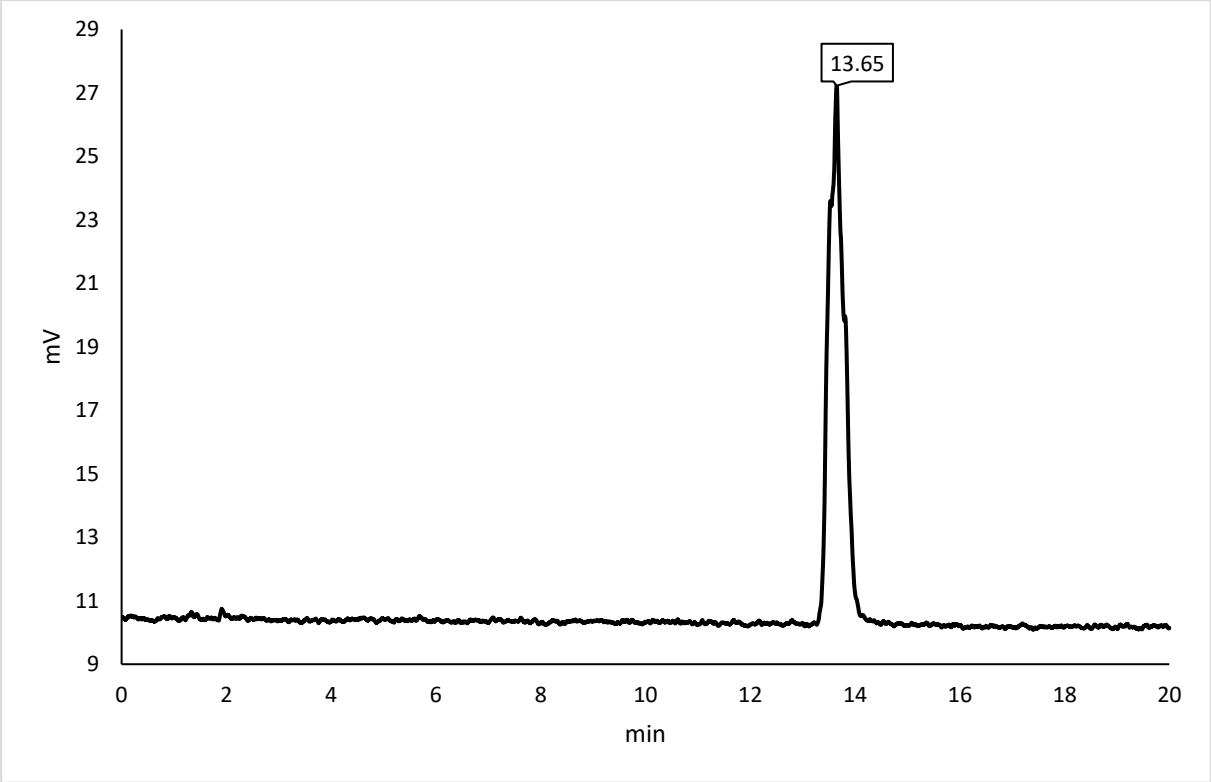

Figure 18: 3F-LacNAc chromatogram - ACN/ammonium acetate buffer (10 mM, pH 6.4) 90:10, sample concentration: 0.25 mg/mL, injection volume: 2 µL, mobile phase flow: 0.3 mL/min, column: Luna Omega 3 µm Sugar 100 Å (150 × 2.1 mm), column temperature: 25 °C, detector: ELSD

In *Figure 18,* different sample concentration was tested compared to the previous chromatograms. Decreasing the sample concentration from 0.5mg/mL to 0.25 mg/mL provided a better peak shape compared to *Figure 17.*

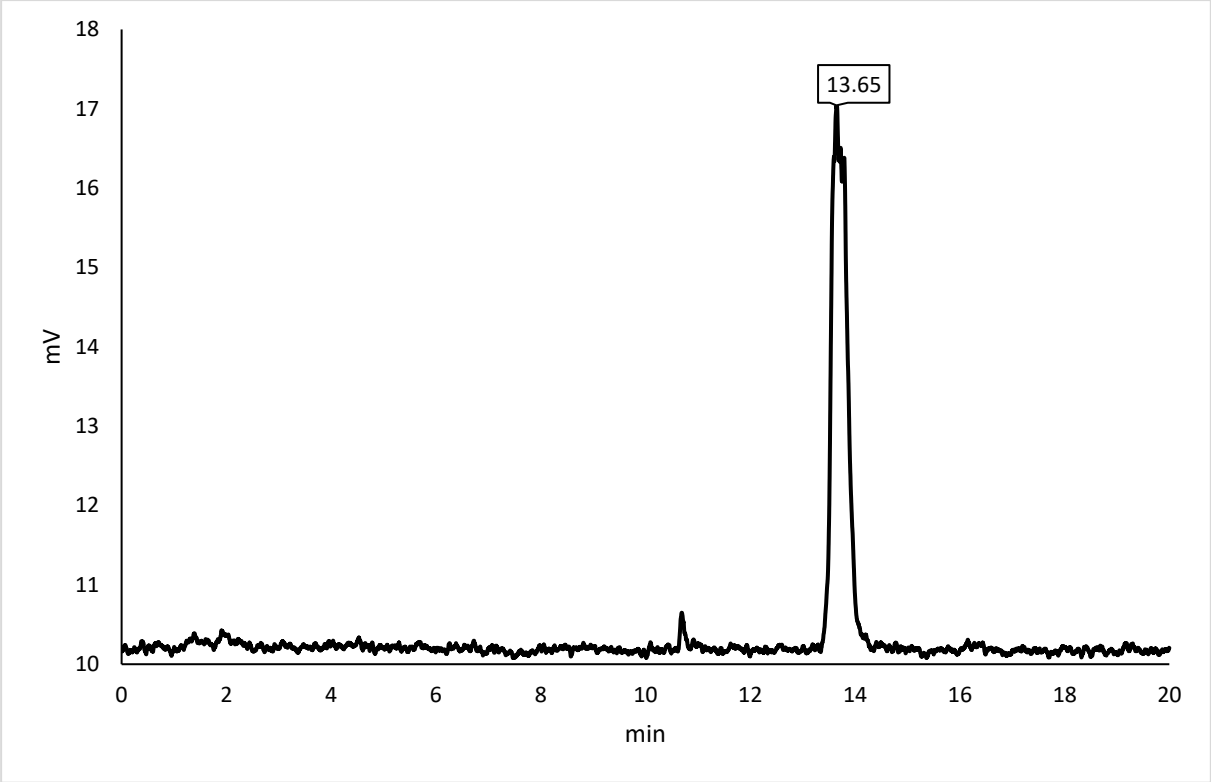

Figure 19: 3F-LacNAc chromatogram - ACN/ammonium acetate buffer (10 mM, pH 6.4) 90:10, sample concentration: 0.125 mg/mL, injection volume: 2 μL, mobile phase flow: 0.3 mL/min, column: Luna Omega 3 μm Sugar 100 Å (150 × 2.1 mm), column temperature: 25 °C, detector: ELSD

Improvement in peak appearance with decreasing concentration (*Figure 18*) led to testing a sample diluted to a concentration of 0.125 mg/mL (*Figure 19*). This dilution did not provide a significant improvement in peak appearance (peak splitting was observed)

The method optimization process focused mainly on two parameters: Peak shape and retention time. Therefore, different injection volumes, sample concentrations and ratios of mobile phase components were investigated. The optimization of the method was carried out on 3F-LacNAc, as it was assumed that its retention time would be the longest due to its highest hydrophilicity of the LacNAc series.[81] Based on the results, **sample concentration** 0.25 mg/mL and **injection volume** 2 μL were chosen. The composition of mobile phase was further optimized using the measurement of the entire series of deoxyfluorinated methyl *N*-acetyl-β-D-lactosaminides.

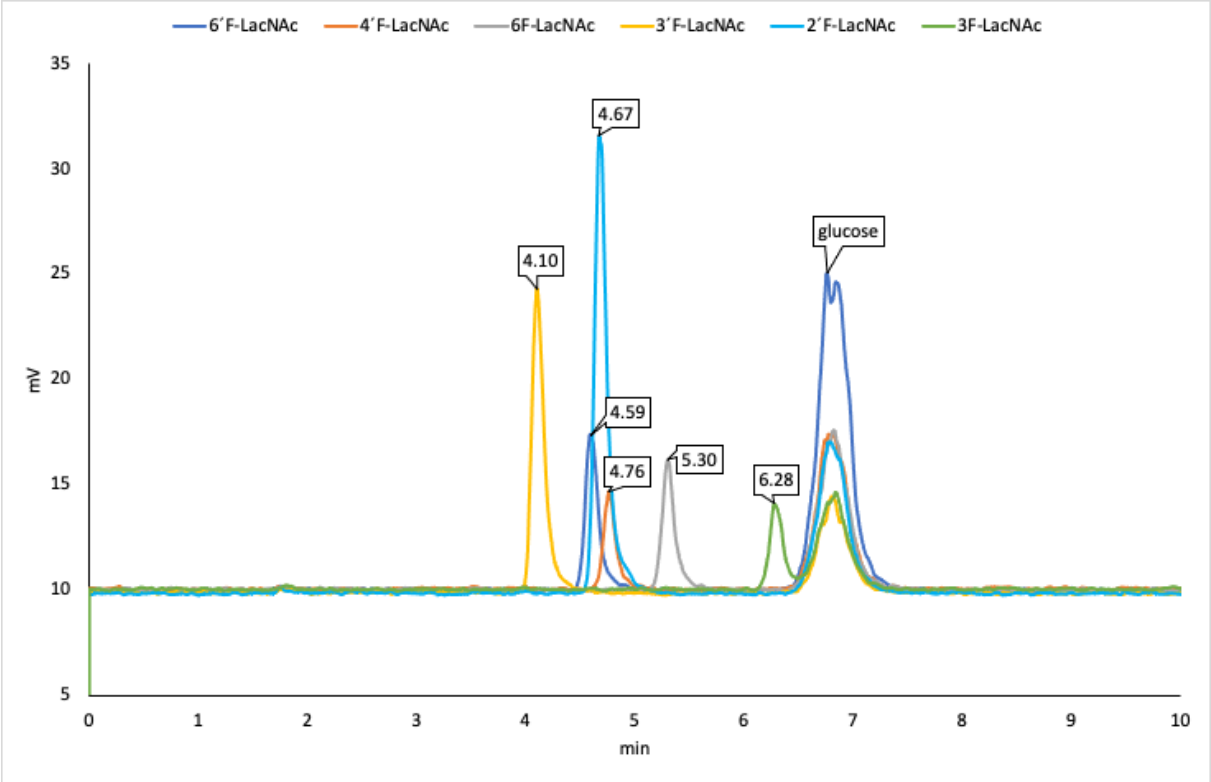

Figure 20: Overlay of chromatograms of LacNAc series - Mobile phase: ACN/ammonium acetate buffer (10 mM, pH 6.4) 85:15, column: Luna Omega 3 µm Sugar 100 Å (150 × 2.1 mm), mobile phase flow: 0.3 mL/min, sample concentration 0.25 mg/mL, injection volume 2 µL, column temperature: 25 °C, detector: ELSD

Figure 20 illustrates that with a mobile phase ratio of 85:15, the signals for the 2′F-LacNAc, 6′F-LacNAc, and 4′F-LacNAc samples overlap significantly. The resolution between these three samples was determined using the following formula[60]

$$R = 1.18\frac{t_{R2}-t_{R1}}{(W_{0.5h1}+W_{0.5h2})} \quad (14)$$

Where t_{R2} [min], t_{R1}[min] are retention times for each peak and W_1 [min], W_2 [min] are full width at half maximum of each peak.

R (6′F, 2′F) = 0.400

R (2′F, 4′F) = 0.442

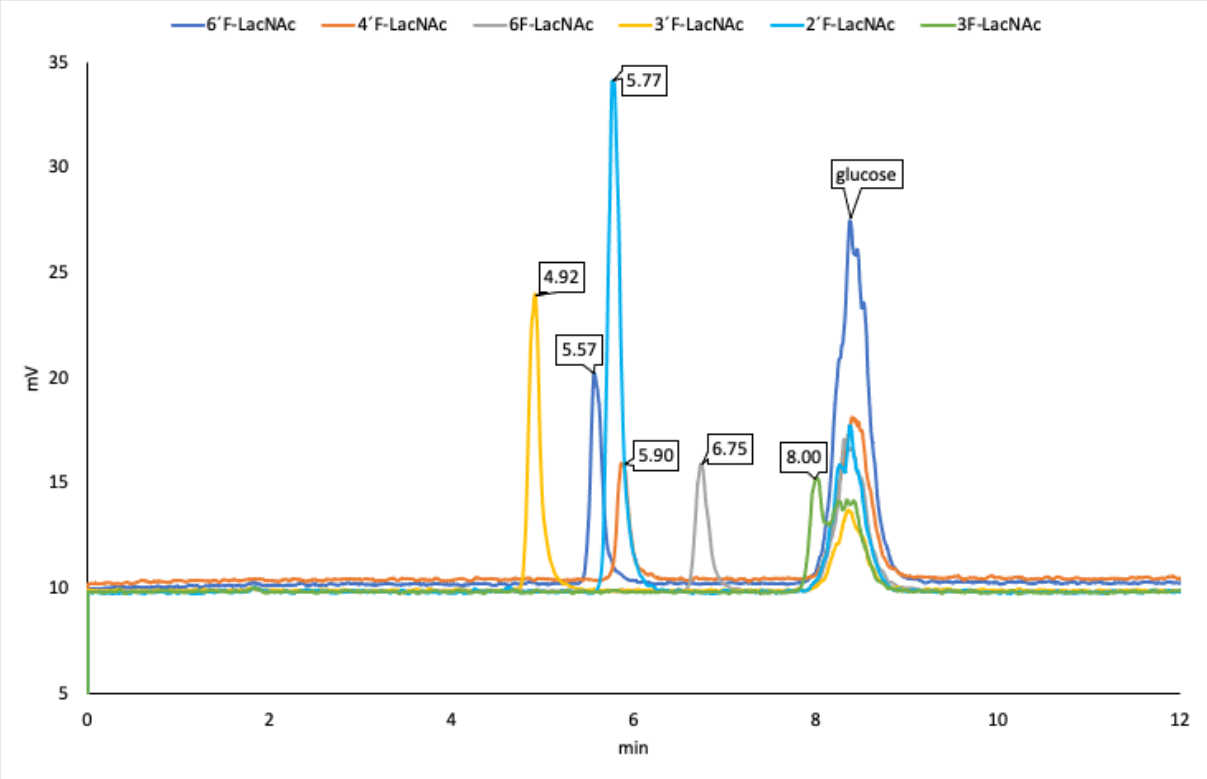

Figure 21: Overlay of chromatograms of LacNAc series - Mobile phase ACN/ammonium acetate buffer (10 mM, pH 6.4) 87:13, column: Luna Omega 3 µm Sugar 100 Å (150 × 2.1 mm), mobile phase flow: 0.3 mL/min, sample concentration 0.25 mg/mL, injection volume 2 µL, column temperature: 25 °C, detector: ELSD

The resolution of 2′F-LacNAc and 6′F-LacNAc improved when using a mobile phase with an 87:13 ratio, as illustrated in *Figure 21*. For 2′F-LacNAc and 4′F-LacNAc, the resolution remained nearly the same. With this mobile phase, there was a significant signal overlap between 3F-LacNAc and the internal standard compound.

R (6′F, 2′F) = 0.810

R (2′F, 4′F) = 0.413

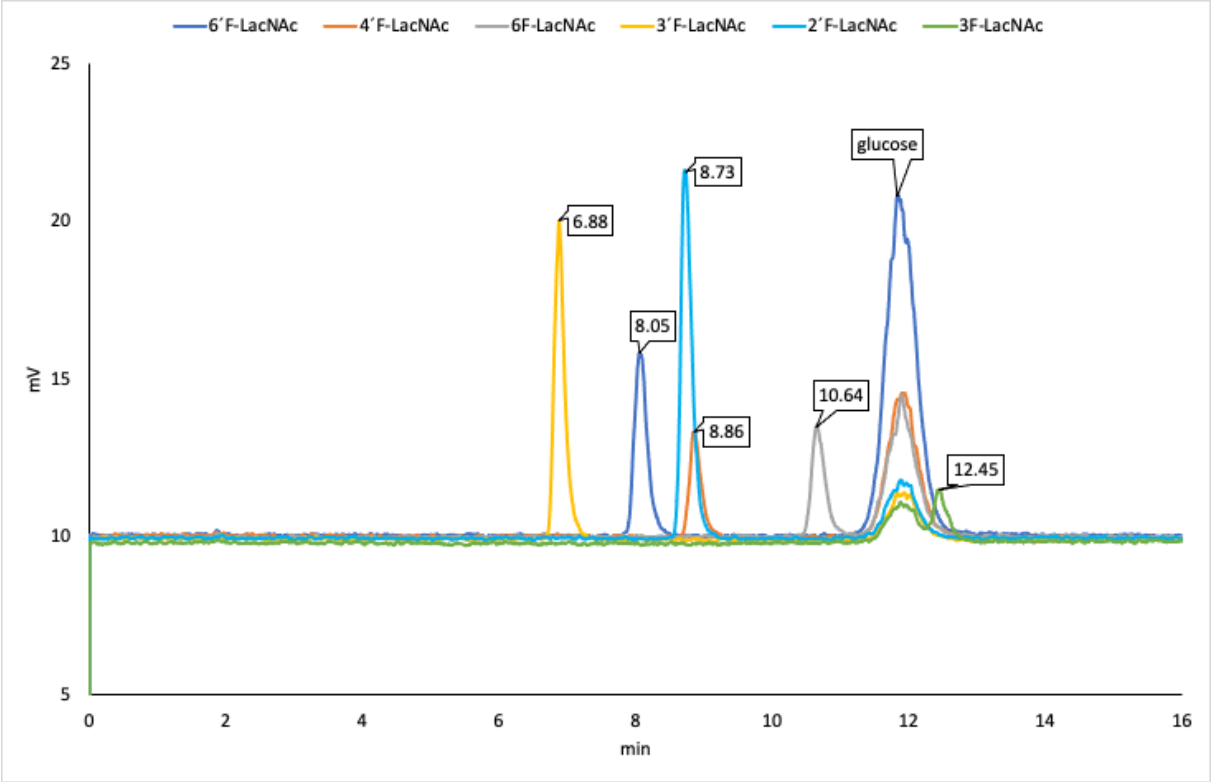

Figure 22: Overlay of chromatograms of LacNAc series - Mobile phase ACN/ammonium acetate buffer (10 mM, pH 6.4) 90:10, column: Luna Omega 3 µm Sugar 100 Å (150 × 2.1 mm), mobile phase flow: 0.3 mL/min, sample concentration 0.25 mg/mL, injection volume 2 µL, column temperature: 25 °C, detector: ELSD

Since increasing the acetonitrile concentration from 85% to 87% enhanced the resolution, the mobile phase with 90:10 ratio was also tested. Using this 90:10 ratio significantly improved the resolution between 2′F-LacNAc and 6'F-LacNAc, while the resolution of 2′F-LacNAc and 4′F-LacNAc was not affected (*Figure 22).* Therefore, 90:10 was evaluated as optimal for our purpose and no alternative mobile phase ratio was investigated. *Figure 22* also illustrates a noticeable decrease in the intensity of individual peaks caused by the gradual fouling of the ELSD detector, as discussed above in this chapter. This is particularly evident in the chromatogram of 3F-LacNAc, which was acquired as the last in the series.

R (6′F, 2′F) = 2.077

R (2′F, 4′F) = 0.423

5.2.2 Optimized measurement

Conditions:

Column: Luna Omega 3 µm Sugar 100 Å, 150 x 2.1 mm

Mobile phase: ACN/10mM ammonium acetate, pH 6.4 (90/10 v/v)

Stationary phase: silica gel coated amine amide-Polyol functions

Elution mode: Isocratic

Internal standard: methyl β-D-glucopyranoside

Mobile phase flow: 0.3 mL/min

Injected volume: 2 µL

Sample concentration ~ 0.025 mg/mL

Under optimized chromatographic conditions, retention of compounds in Lac and LacNAc series on a HILIC column were determined, using MS-ESI detection. Each measurement was repeated three times (*Table 1* and *Table 2*) and the retention times were averaged. *Table 1* shows average retention times of deoxyfluorinated methyl β-D-lactosides ($\bar{t}_R^s$), average retention times for internal standard methyl β-D-glucopyranoside ($\bar{t}_R^{st}$) and corresponding standard deviation (SD) and relative standard deviations (RSD). Acquired data indicate a relatively low RSD for all samples, proving a good repeatability of the method.

Table 1: Average retention times for Lac series with absolute and relative standard deviations

Sample	$\bar{t}_R^s$ min	$\bar{t}_R^{st}$ min	SD_{sample}	$SD_{standard}$	RSD_{sample} %	$RSD_{standard}$ %
3′F	5.878	5.282	0.011	0.019	0.187	0.361
6′F	6.186	5.217	0.017	0.014	0.233	0.268
2F	6.369	5.249	0.043	0.023	0.677	0.447
4′F	6.853	5.272	0.001	0.006	0.008	0.120
2′F	7.259	5.255	0.017	0.014	0.233	0.268
6F	8.446	5.257	0.003	0.009	0.031	0.176
3F	8.896	5.264	0.018	0.007	0.204	0.126

Similarly, *Table 2* displays the average retention times for methyl *N*-acetyl-β-D-lactosaminides average retention times for internal standard methyl β-D-glucopyranoside ($\bar{t}_R^{st}$) and corresponding standard deviation (SD) and relative standard deviations (RSD). This data also indicates a relatively low RSD for all samples (although on average the deviations were greater than in the Lac series), proving a good repeatability of the method.

Table 2: Averaged retention times for LacNAc series with absolute and relative standard deviations

Sample	$\bar{t}_R^s$ min	$\bar{t}_R^{st}$ min	SD_{sample}	$SD_{standard}$	RSD_{sample} %	$RSD_{standard}$ %
3′F	6.569	5.240	0.014	0.011	0.214	0.210
6′F	7.551	5.208	0.081	0.036	1.072	0.690
2′F	8.074	5.214	0.088	0.022	1.089	0.414
4′F	8.247	5.235	0.006	0.010	0.077	0.187
6F	9.770	5.229	0.038	0.010	0.391	0.193
3F	11.437	5.217	0.047	0.034	0.412	0.655

Figure 23 shows the chromatogram with retention times of Lac analogs, with t_R from 5.88 to 8.90 minutes. Generally, hydrophilic substances should exhibit longer retention times on the HILIC column compared to hydrophobic substances.[60] The data obtained for Lac series are in partial agreement with the above-mentioned stir-flask method with ^{19}F NMR detection. Both stir-flask and HILIC methods show 3F-Lac (t_R = 8.90 min, log P = − 3.45) and 6F-Lac (t_R = 8.45 min, log P = −3.26) analogs as the most hydrophilic substances. Similarly, the 4′F-Lac (t_R = 6.85, log P = −3.20) holds the middle position in the series according to both methods of lipophilicity determination, when compounds are arranged in the order of increasing lipophilicity values. However, 3'F-Lac has the shortest retention time (t_R = 5.88 min, log P = −3.13), although its lipophilicity is not the highest. Similarly, 6′F-Lac (t_R = 6.19 min, log P = −3.22) does not align with the expectation that it should have the third longest retention time; instead, it has the second shortest.

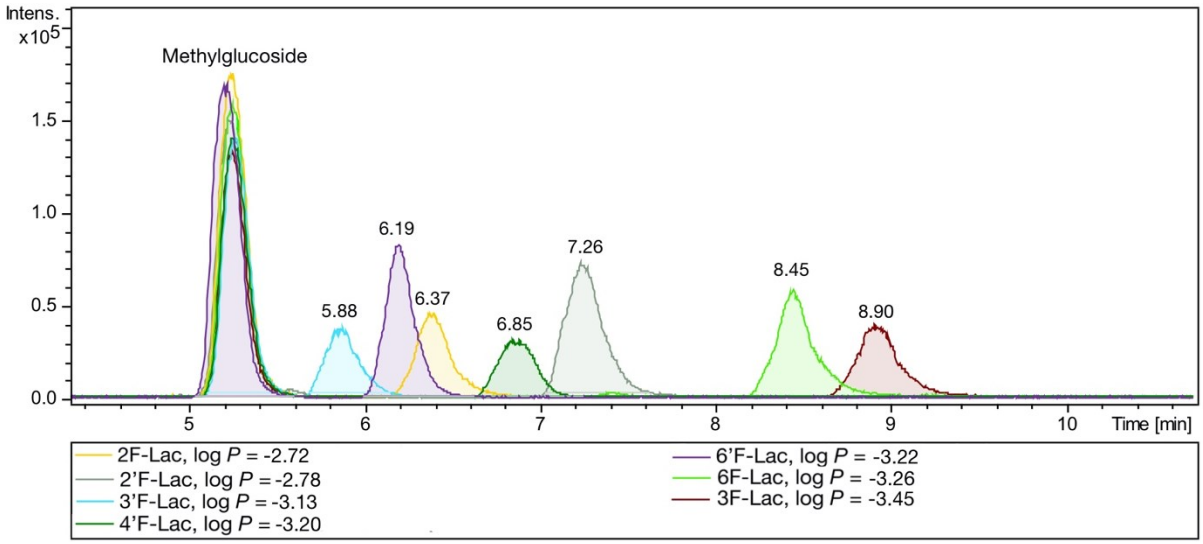

Figure 23: Retention times of deoxyfluorinated methyl β-D-lactosides. Mobile phase ACN/ammonium acetate buffer (10 mM, pH 6.4) 90:10, column: Luna Omega 3 µm Sugar 100 Å (150 × 2.1 mm), mobile phase flow: 0.3 mL/min, sample concentration 0.025 mg/mL, injection volume 2 µL, column temperature: 25 °C, detector: ESI-MS

Similar results are shown in *Figure 24* with the retention times of LacNAc series. Retention times for LacNAc series are a bit longer, with larger differences than for Lac series (with t_R from 6.57 to 11.43 minutes, Table 2). Again, these data are in partial agreement with the results of the NMR method. Both methods identified 3F-LacNAc (t_R = 11.43 min, log P = −3.45) the most hydrophilic substance in LacNAc series. Both methods also agree for the 4′F (t_R = 8.25, log P = −3.10) analog, identifying it as the third most hydrophilic compound in the series. Further correlation between NMR and HILIC methods is not entirely clear. For example, 2'F-LacNAc has the third shortest retention time (t_R = 8.07 min, log P = −2.92), although its lipophilicity is the highest. Similarly, 6F-LacNAc (t_R = 9.77 min, log P = −2.95) does not align with the expectation that it should have the second shortest retention time; instead, it has the second longest. 3′F-LacNAc also does not match with its shortest retention time to determined log P (t_R = 6.57 min, log P = −3.09).

Notably, there is a strong correlation between the HILIC retention times of individual compounds of Lac and LacNAc series (*Figure 25*), emphasizing the structural similarities between both saccharide systems. 3′F analogs have the shortest t_R, 6′F analogs have the second

shortest t_R. The longest retention time t_R is observed for 3F analogs, and the second longest is for the 6F analogs.

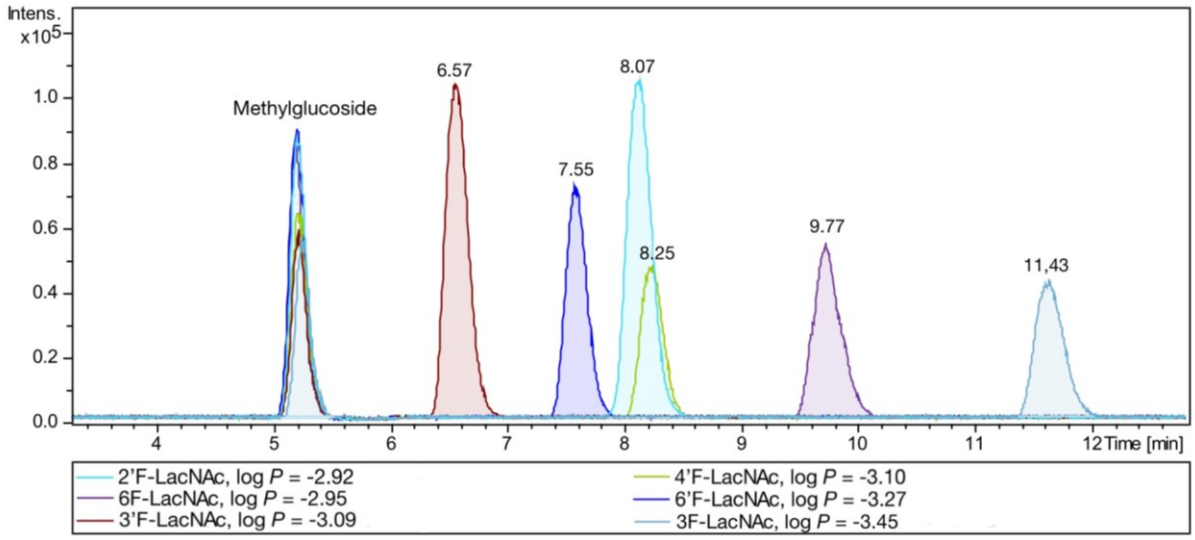

Figure 24: Retention times of deoxyfluorinated methyl *N*-acetyl-β-D-lactosaminide series. Mobile phase ACN/ammonium acetate buffer (10 mM, pH 6.4) 90:10, column: Luna Omega 3 µm Sugar 100 Å (150 × 2.1 mm), mobile phase flow: 0.3 mL/min, sample concentration 0.025 mg/mL, injection volume 2 µL, column temperature: 25 °C, detector: ESI-MS

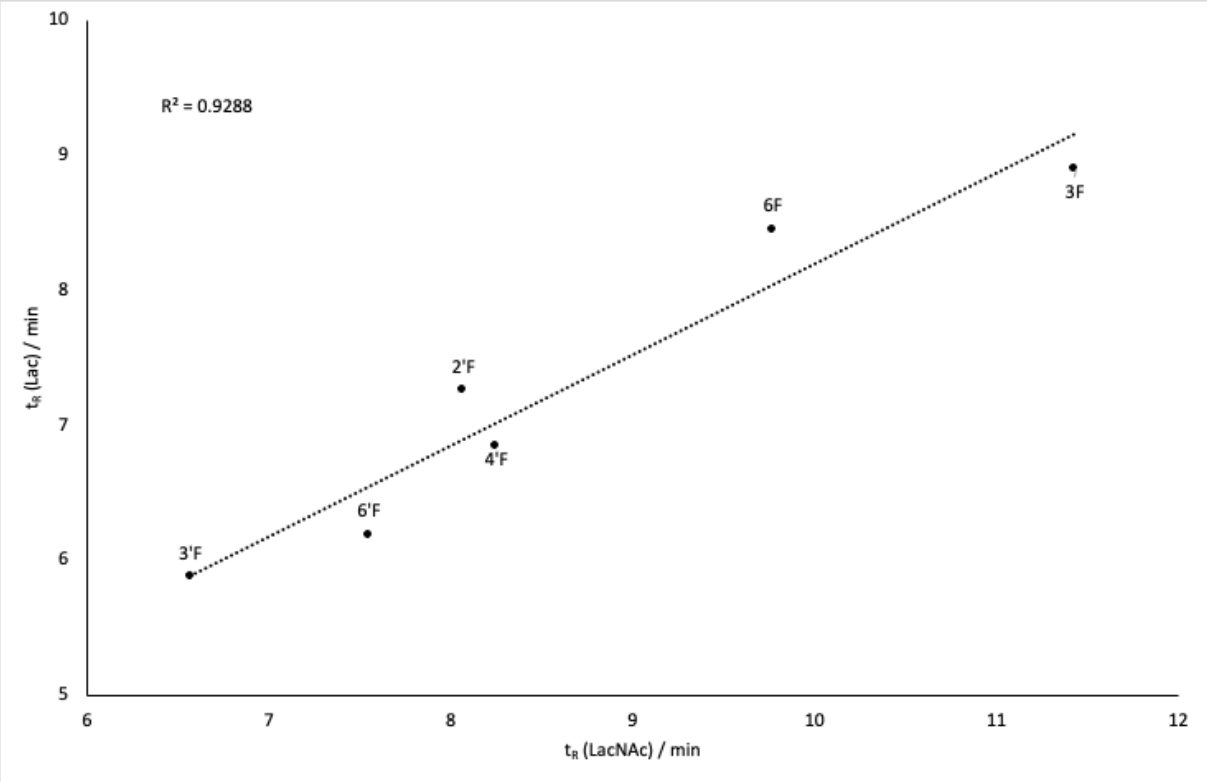

Figure 25: Correlation of retention times of the Lac and LacNAc series.

5.3 Results of COSMO-RS prediction

It was recently reported that the COSMO-RS method can accurately predict lipophilicities of deoxyfluorinated methyl *N*-acetyl-β-D-lactosaminides.[85] Encouraged by these results, I was interested whether COSMO-RS method enables to identify lipophilicity trends associated with individual deoxyfluorinations of methyl β-D-lactosides (Lac).

For most of the deoxyfluorinated methyl β-D-lactosides, the COSMO-RS prediction agreed well with the stir-flask method (^{19}F NMR detection) (*Table 3, Figure 26*). Both methods indicate that 3F-Lac is the least lipophilic compound in the series, which also agrees with the determination by HILIC (*Table 1*). Similarly, both COSMO-RS prediction and the stir-flask method identified 2F-Lac and 2′F-Lac as the first and the second most lipophilic compounds in the series, respectively. Also, log *P* values of 3′F-Lac and 4′F-Lac showed a good agreement between prediction and experimental determination, although their relative positions within the series were incorrectly predicted.

Table 3: Log *P* values of deoxyfluorinated methyl β-D-lactosides obtained by COSMO-RS prediction and experimental stir-flask method with ^{19}F NMR detection.

	3F	**6F**	**6′F**	**4′F**	**3′F**	**2′F**	**2F**
Log $P_{COSMO\text{-}RS}$	−3.76	−2.58	−2.72	−3.25	−3.01	−2.45	−2.29
Log P_{NMR}	−3.45	−3.26	−3.22	−3.20	−3.13	−2.78	−2.72

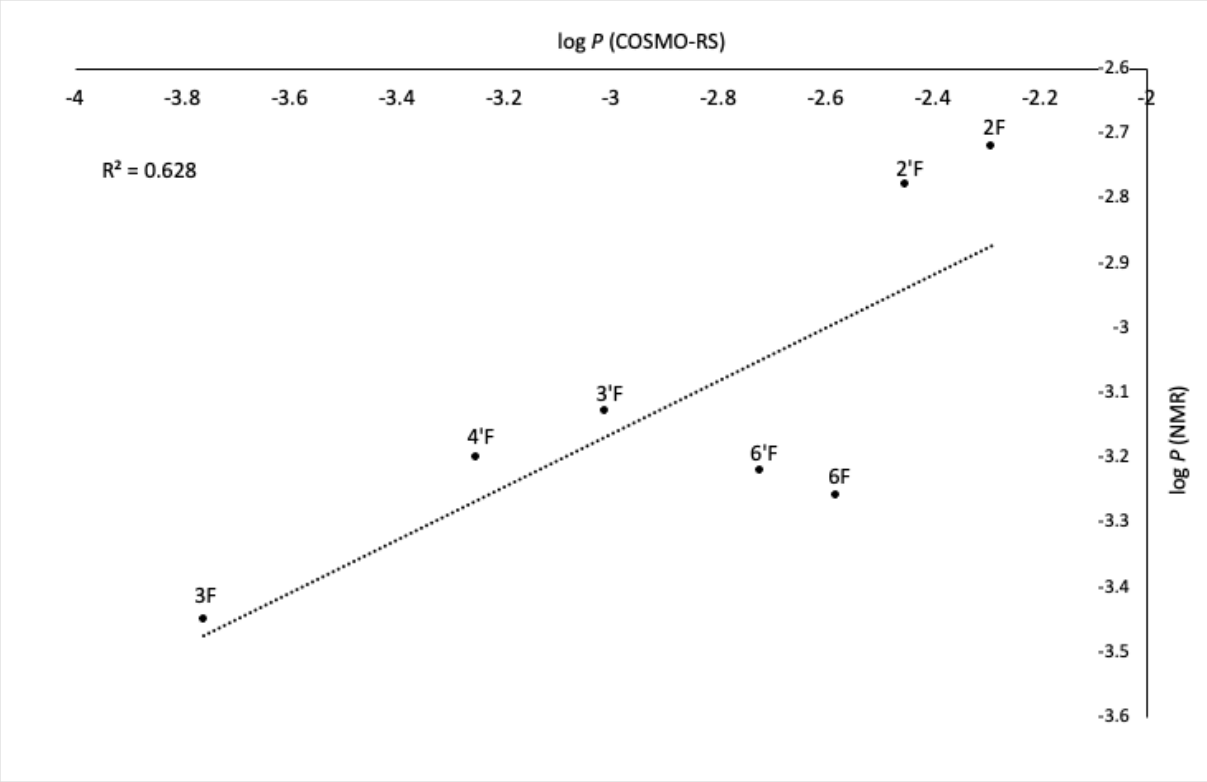

Figure 26: Correlation of predicted (COSMO-RS) and experimentally determined (stir-flask with ^{19}F NMR detection) log *P* values of deoxyfluorinated methyl β-D-lactosides.

COSMO-RS method, however, overestimated the lipophilicity of 6F-Lac and 6′F-Lac, providing significantly higher log *P* values compared to the stir-flask determination. These data illustrate limitations of the COSMO-RS method in lipophilicity prediction. Observed discrepancy is likely caused by the simplicity of our prediction model, which takes only the most stable conformer into account. Flexible molecules such as β(1→4)-linked D-lactose analogs frequently show the presence of multiple conformational states in solution. These conformers can have significantly different σ-profiles and log *P* values, which complicate the

prediction of lipophilicity by COSMO-RS.[87] But despite the small difference in log *P* values, COSMO-RS was able to predict log *P* for most compounds. Therefore, it can be advantageously used as a method to tentatively estimate log *P* of fluorinated oligosaccharides.

6. Conclusion

All objectives of this thesis were fulfilled. Initially, lipophilicity expressed as log *P* was determined for the series of deoxyfluorinated methyl β-D-galactosides and deoxyfluorinated methyl β-D-lactosides by the stir-flask method with ^{19}F NMR detection. For D-galactoside series, 3F-Galβ1-OMe showed the highest lipophilicity (log *P* = −1.42) while 4F-Galβ1-OMe showed the lowest lipophilicity of the series (log *P* = −2.06). The remaining compounds 2F-Galα1-OMe, 2F-Galβ1-OMe, 6F-Galβ1-OMe had very similar lipophilicities. In Lac series 3F-Lac showed the lowest lipophilicity (log *P* = −3.45). The compounds 6F-Lac, 6′F-Lac, 4′F-Lac and 3′F-Lac showed very similar lipophilicities (log *P* from −3.26 to −3.13). 2′F-Lac (log *P* = −2.78) and 2F-Lac (log *P* = −2.72) have the highest lipophilicity of Lac series. Determined trends in lipophilicity were in strong agreement with previously reported data of structurally related deoxyfluorinated methyl *N*-acetyl-β-D-lactosaminides.[81] These results agree with the previously reported hypothesis that the low relative lipophilicity of 3F-LacNAc is caused by the presence of $O5 \cdots H - O3$ hydrogen bond in its structure. The hydroxyl OH-3 is involved as a donor of this hydrogen bond, which reduces its solvation compared to other hydroxyl groups. Consequently, deoxyfluorination of OH-3 does not increase log *P* to the same extent as deoxyfluorination at other positions.[85]

Furthermore, I developed an alternative method for estimating the lipophilicity of mono deoxyfluorinated disaccharides using hydrophilic interaction chromatography with detection by electrospray ionization mass spectrometry (HILIC-ESI-MS). Optimized conditions: Column Luna Omega 3 µm Sugar 100 Å, 150 x 2.1 mm, mobile phase: ACN/10mM ammonium acetate, pH 6.4 (90/10 v/v), isocratic elution, internal standard: methyl β-D-glucopyranoside, mobile phase flow: 0.3 mL/min, injected volume: 2 µL and sample concentration ~ 0.025 mg/mL. The HILIC method is fast, robust, easy to perform, and provided data in qualitative agreement with the stir flask method for following compounds: 3F-Lac, 6F-Lac, and 4′F-Lac. However, for other substances, the method unfortunately provided a different relative order of lipophilicity. This can be attributed to the different principles of the two methods. Further research in this area is necessary to explain the observed phenomena.

Finally, the obtained log *P* values were compared to the values predicted by the COSMO-RS method. This method showed a partial correlation with the stir-flask method (^{19}F NMR

detection) for Lac series. Both methods indicate that 3F-Lac is the least lipophilic compound in the series and similarly, both identified 2F-Lac and 2′F-Lac as the first and the second most lipophilic compounds in the series. Also, log *P* values of 3′F-Lac and 4′F-Lac showed a good agreement between prediction and experimental determination. However, COSMO-RS provided significantly higher log *P* values for 6F-Lac and 6′F-Lac, compared to the stir-flask determination. Therefore, although COSMO-RS method has a great ability to estimate the log *P* values of fluorinated oligosaccharides, its results should be interpreted with caution.

7. Acknowledgment

In conclusion, I want to express my gratitude to Ing. Martin Kurfiřt for his invaluable guidance and patience during both the experimental part and the thesis writing process. I also appreciate Ing. Jana Bernášková, Ph.D. for instructing me on the use of analytical instruments and offering essential advice during measurements. My thanks extend to doc. RNDr. Martin Dračínský for granting me access to the NMR spectrometer at the Institute of Organic Chemistry and Biochemistry of the CAS, as well as to Ing. Martin Balouch, Ph.D. for conducting COSMO-RS calculations. I am also thankful to all members of the Research Group of Bioorganic Chemistry and Biochemistry at the Institute of Chemical Process Fundamentals of the CAS, who consistently fostered a welcoming working atmosphere that I enjoyed returning to, and who provided valuable input during my laboratory work. Additionally, I wish to thank Mgr. Jinřich Karban, Ph.D. for including me in the project and offering insightful advice regarding my thesis. Finally, I'd like to thank doc. RNDr. Petr Kozlík, Ph.D. for overseeing my thesis, its revisions, and for his valuable insights.

I want to extend my gratitude to my family for their unwavering support and trust during my studies. A special thank you goes to my mother, who has always been my unconditional supporter in pursuing my goals. I would also like to thank my boyfriend for his unconditional support.

8. References

(1) Linclau, B.; Wang, Z.; Compain, G.; Paumelle, V.; Fontenelle, C. Q.; Wells, N.; Weymouth-Wilson, A. Investigating the Influence of (Deoxy)Fluorination on the Lipophilicity of Non-UV-Active Fluorinated Alkanols and Carbohydrates by a New Log P Determination Method. *Angewandte Chemie - International Edition, 55* (2), 674–678 (2016). https://doi.org/10.1002/anie.201509460

(2) Waring, M. J. Lipophilicity in Drug Discovery. *Expert Opinion on Drug Discovery*, *5* (3), 235–248, (2010). https://doi.org/10.1517/17460441003605098.

(3) Inoue, M.; Sumii, Y.; Shibata, N. Contribution of Organofluorine Compounds to Pharmaceuticals. *ACS Omega*, *5* (19), 10633–10640, (2020). https://doi.org/10.1021/acsomega.0c00830.

(4) Wei, X.; Wang, P.; Liu, F.; Ye, X.; Xiong, D. Drug Discovery Based on Fluorine-Containing Glycomimetics. *Molecules*, *28* (18), (2023). https://doi.org/10.3390/molecules28186641.

(5) Hevey, R. The Role of Fluorine in Glycomimetic Drug Design. *Chemistry - A European Journal*, *27* (7), 2240–2253, (2021). https://doi.org/10.1002/chem.202003135.

(6) Jiménez-Barbero, J.; Linclau, B.; Ardá, A.; Reichardt, N. C.; Sollogoub, M.; Unione, L.; Vincent, S. P. Fluorinated Carbohydrates as Chemical Probes for Molecular Recognition Studies. Current Status and Perspectives. *Chemical Society Reviews*, *49* (12), 3863–3888, (2020), https://doi.org/10.1039/c9cs00099b.

(7) Leusmann, S.; Ménová, P.; Shanin, E.; Titz, A.; Rademacher, C. Glycomimetics for the Inhibition and Modulation of Lectins. *Chemical Society Reviews*, *52* (11), 3663–3740, (2023). https://doi.org/10.1039/d2cs00954d.

(8) Hansch, C.; Fujita, T. ρ-σ-π Analysis. A Method for the Correlation of Biological Activity and Chemical Structure. *Journal of the American Chemical Society*, *86* (24), 5710, (1964). https://doi.org/10.1021/ja01078a623.

(9) Asif, H.; Akram, M.; Saeed, T.; Khan, M.; Akhtar, N.; Rehman, R.; Shah, S.; Ahmed, K.; Shaheen, G. Review Paper : Carbohydrates. *International Research Journal of Biochemistry and Bioinformatics*, *1* (1), 1–5, (2011).

(10) Kodíček, M.; Valentová, O.; Hynek, R. Biochemie: Chemický Pohled Na Biologický Svět, VŠCHT, (2018).

(11) McNaught, A. D. Nomenclature of Carbohydrates. *Pure and Applied Chemistry*, *68* (10), 1919–2008, (1996).

(12) Varki, A.; Cummings, R. D.; Esko, J. D.; Stanley, P.; Hart, G. W.; Aebi, M.; Mohnen, D.; Kinoshita, T.; Packer, N. H.; Prestegard, J. H.; Schnaar, R. L.; Seeberger, P. H. Essentials of Glycobiology*,* 4th ed.; Cold Spring Harbor Laboratory Press, U.S., (2022). https://doi.org/10.1101/9781621824213.

(13) Tamburrini, A.; Colombo, C.; Bernardi, A. Design and Synthesis of Glycomimetics: Recent Advances. *Medicinal Research Reviews*, *40* (2), 495–531, (2019). https://doi.org/10.1002/med.21625.

(14) Naresh, P.; Jubie, S.; Prabha, T.; Shyam Sundar, P.; Santhosh, S. B. A Brief Review on Glycomimetics and Their Pharmaceutical Applications. *International Journal of Pharmaceutical Sciences and Research*, *11* (7), 1000–1009, (2020). https://doi.org/10.13040/IJPSR.0975-8232.11(7).3078-86.

(15) O'hagan, D. Understanding Organofluorine Chemistry. An Introduction to the C–F Bond. *Chemical Society Review*, *37* (2), 308–319, (2008). https://doi.org/10.1039/b711844a.

(16) Uhrig, M. L.; Lantaño, B.; Postigo, A. Synthetic Strategies for Fluorination of Carbohydrates. *Organic and Biomolecular Chemistry*, *17* (21), 5173–5189, (2019). https://doi.org/10.1039/c9ob00405j.

(17) Wang, Q.; Guo, Z. Synthetic and Immunological Studies of STn Derivatives Carrying Substituted Phenylacetylsialic Acids as Cancer Vaccine Candidate. *ACS Medicinal Chemistry Letters*, *2* (5), 373–378, (2011). https://doi.org/10.1021/ml100313d.

(18) Wang, J.; Li, H.; Zou, G.; Wang, L. X. Novel Template-Assembled Oligosaccharide Clusters as Epitope Mimics for HIV-Neutralizing Antibody 2G12. Design, Synthesis, and Antibody Binding Study. *Organic and Biomolecular Chemistry*, *5* (10), 1529–1540, (2007). https://doi.org/10.1039/b702961f.

(19) Som, P.; Atkins, H. L.; Bandoypadhyay, D.; Fowler, J. S.; Macgregor, A. R.; Matsui, K.;

Oster, Z. H.; Sacker, D. F. A Fluorinated Glucose Analog , 2-Fluoro-2-Deoxy-D-Glucose (F-18): Nontoxic Tracer for Rapid Tumor Detection. *Journal of Nuclear Medicine*, *21* (7), 670–675, (1980).

(20) Rutkowska, E.; Pajak, K.; Jozwiak, K. Lipophilicity - Methods of Determination and Its Role in Medicinal Chemistry. *Acta Poloniae Pharmaceutica*, *70*, 3–18, (2012).

(21) Everett, D. H.; Butterworths, L. Manual of Symbols and Terminology for Physicochemical Quantities and Units, Appendix II: Definitions, Terminology and Symbols in Colloid and Surface Chemistry. *Pure and Applied Chemistry*, *34*, 577–638, (1971).

(22) Di, L.; Kerns, E. H. Lipophilicity. *Drug-Like Properties*, 39–50, (2016). https://doi.org/10.1016/b978-0-12-801076-1.00005-8.

(23) Rosenkranz, H. S.; Matthews, E. J.; Klopman, G. Relationships between Cellular Toxicity, the Maximum Tolerated Dose, Lipophilicity and Electrophilicity. *Alternatives to Laboratory Animals*, *20* (4), 549–562, (1992). https://doi.org/10.1177/026119299202000407.

(24) Herrmann, T.; Leavitt, L.; Sharma, S. Physiology, Membrane.; Treasure Island (FL), 2023.

(25) Arnott, J. A.; Kumar, R.; Planey, S. L. Lipophilicity Indices for Drug Development. *Journal of Applied Biopharmaceutics and Pharmacokinetics*, *1*, 31–36, (2013). https://doi.org/10.14205/2309-4435.2013.01.01.6.

(26) Chmiel, T.; Mieszkowska, A.; Kempińska-Kupczyk, D.; Kot-Wasik, A.; Namieśnik, J.; Mazerska, Z. The Impact of Lipophilicity on Environmental Processes, Drug Delivery and Bioavailability of Food Components. *Microchemical Journal*, *146*, 393–406, (2018). https://doi.org/10.1016/j.microc.2019.01.030.

(27) Abla, M. J.; Banga, A. K. Quantification of Skin Penetration of Antioxidants of Varying Lipophilicity. *International Journal of Cosmetics Science*, *35* (1), 19–26, (2013). https://doi.org/10.1111/j.1468-2494.2012.00728.x.

(28) Ginex, T.; Vazquez, J.; Gilbert, E.; Herrero, E.; Luque, F. J. Lipophilicity in Drug Design: An Overview of Lipophilicity Descriptors in 3D-QSAR Studies. *Future*

Medicinal Chemistry, *11* (10), 1177–1193, (2019). https://doi.org/10.4155/fmc-2018-0435.

(29) Leahy, D. E.; Taylor, P. J.; Wait, A. R.; Park, A. Model Solvent Systems for QSAR Part I. Propylene Glycol Dipelargonate (PGDP). A New Standard Solvemt for Use in Partition Coefficient Determination. *Molecular Informatics*, *31*, 17–31, (1989).

(30) Hattotuwagama, C. K.; Flower, D. R. Empirical Prediction of Peptide Octanol-Water Partition Coefficients. *Bioinformation*, *1* (7), 257–259, (2006). https://doi.org/10.6026/97320630001257.

(31) Kah, M.; Brown, C. D. Log D: Lipophilicity for Ionisable Compounds. *Chemosphere*, *72* (10), 1401–1408, (2008). https://doi.org/10.1016/j.chemosphere.2008.04.074.

(32) Lipinski, C. A.; Lombardo, F.; Dominy, B. W.; Feeney, P. J. Experimental and Computational Approaches to Estimate Solubility and Permeability in Drug Discovery and Development Settings. *Advanced Drug Delivery Reviews*, *64*, 4–17, (2012). https://doi.org/10.1016/j.addr.2012.09.019.

(33) Buttersack, C. Hydrophobicity of Carbohydrates and Related Hydroxy Compounds. *Carbohydrate Research*, *446–447*, 101–112, (2017). https://doi.org/10.1016/j.carres.2017.04.019.

(34) Saha, S.; Dilipkumar, P. Log P. *Encyclopedia of Physical Organic Chemistry*, 1–22, (2017).

(35) Danielsson, L. G.; Zhang, Y. H. Methods for Determining N-Octanol-Water Partition Constants. *Trends in Analytical Chemistry*, *15* (4), 188–196, (1996). https://doi.org/10.1016/0165-9936(96)00003-9.

(36) Andrés, A.; Rosés, M.; Ràfols, C.; Bosch, E.; Espinosa, S.; Segarra, V.; Huerta, J. M. Setup and Validation of Shake-Flask Procedures for the Determination of Partition Coefficients (Log D) from Low Drug Amounts. *European Journal of Pharmaceutical Sciences*, *76*, 181–191, (2015). https://doi.org/10.1016/j.ejps.2015.05.008.

(37) OECD/OCDE. Test No. 107: Partition Coefficient (n-Octanol/Water): Shake Flask Method. *Giudance*, *107*, 1–4, (1995).

(38) Krämer, S. D.; Gautier, J. C.; Saudemon, P. Considerations on the Potentiometric Log P

Determination. *Pharmaceutical Research*, 15 (8) 1310–1313, (1998). https://doi.org/10.1023/A:1011968630713.

(39) Valkó, K. Application of High-Performance Liquid Chromatography Based Measurements of Lipophilicity to Model Biological Distribution. *Journal of Chromatography A*, *1037* (1–2), 299–310, (2004). https://doi.org/10.1016/j.chroma.2003.10.084.

(40) Komsta, Ł.; Skibiński, R.; Berecka, A.; Gumieniczek, A.; Radkiewicz, B.; Radoń, M. Revisiting Thin-Layer Chromatography as a Lipophilicity Determination Tool-A Comparative Study on Several Techniques with a Model Solute Set. J*ournal of Pharmaceutical and Biomedical Analysis. 53* (4), 911–918, (2010). https://doi.org/10.1016/j.jpba.2010.06.024.

(41) Soares, J. X.; Santos, Á.; Fernandes, C.; Pinto, M. M. M. Liquid Chromatography on the Different Methods for the Determination of Lipophilicity: An Essential Analytical Tool in Medicinal Chemistry. *Chemosensors*, *10* (8), (2022). https://doi.org/10.3390/chemosensors10080340.

(42) Di, L.; Kerns, E. H. Lipophilicity Methods. *Drug-Like Properties,* 299–306, (2016). https://doi.org/10.1016/b978-0-12-801076-1.00023-x.

(43) Hansch, C.; Hoekman, D.; Gao, H. Comparative QSAR: Toward a Deeper Understanding of Chemicobiological Interactions. *Chemical Reviews*, *96* (3), 1045–1075, (1996). https://doi.org/10.1021/cr9400976.

(44) Klamt, A.; Eckert, F. COSMO-RS: A Novel and Efficient Method for the a Priori Prediction of Thermophysical Data of Liquids. *Fluid Phase Equilibria*, *172* (1), 43–72, (2000). https://doi.org/10.1016/S0378-3812(00)00357-5.

(45) Zloh, M. NMR Spectroscopy in Drug Discovery and Development: Evaluation of Physico-Chemical Properties. *ADMET and DMPK*, *7* (4), 242–251, (2019). https://doi.org/10.5599/admet.737.

(46) Bottomley, P. A. NMR in Medicine. *Computaterized Radiology*, *8* (2), 57–77, (1984). https://doi.org/10.1016/0730-4862(84)90065-9.

(47) Raja, P. M. V; Barron, A. R. Physical Methods in Chemistry and Nano Science. *Journal*

of the Society of Chemical Industry, 335–387, (1934). https://doi.org/10.1002/jctb.5000533702.

(48) Dračínský, M. NMR Spektroskopie pro Chemiky. 2021.

(49) Řezanka, P.; Tkadlecová, M.; Havlíček, J. Nukleární Magnetická Rezonance (NMR). *2* (4).

(50) Hoult, D. I.; Bhakar, B. NMR Signal Reception: Virtual Photons and Coherent Spontaneous Emission. *Concepts in Magnetic Resonance, 9* (5), 277–297, (1997). https://doi.org/10.1002/(sici)1099-0534(1997)9:5<277::aid-cmr1>3.0.co;2-w.

(51) Gerig, J. . Fluorine NMR. (2001). https://doi.org/10.1201/b18854-161.

(52) Reich, H. J. Fluorine Shifts Overview. *NMR Spectroscopy.* (2020).

(53) Claridge, T.; Nader, A. Quantitative NMR Spectroscopy. *University of Oxford*, 1–8, (2017).

(54) Wang, Z.; Jeffries, B. F.; Felstead, H. R.; Wells, N. J.; Chiarparin, E.; Linclau, B. A New Straightforward Method for Lipophilicity (LogP) Measurement Using 19 F NMR Spectroscopy. *Journal of Visualized Experiments,* 143, 1–6, (2019). https://doi.org/10.3791/58567.

(55) Pauli, G. F.; Jaki, B. U.; Lankin, D. C. Quantitative ^{1}H NMR: Development and Potential of a Method for Natural Products Analysis. *Journal of Natural Products*, *68* (1), 133–149, (2005).

(56) Mo, H.; Balko, K. M.; Colby, D. A. A Practical Deuterium-Free NMR Method for the Rapid Determination of 1-Octanol/Water Partition Coefficients of Pharmaceutical Agents. *Bioorganic Medicinal Chemistry Letters*, *20* (22), 6712–6715, (2010). https://doi.org/10.1016/j.bmcl.2010.08.145.

(57) Soulsby, D.; Chica, J. A. M. Determination of Partition Coefficients Using 1H NMR Spectroscopy and Time Domain Complete Reduction to Amplitude-Frequency Table (CRAFT) Analysis. *Magnetic Resonance in Chemistry*, *55* (8), 724–729, (2017). https://doi.org/10.1002/mrc.4582.

(58) Cumming, H.; Rücker, C. Octanol-Water Partition Coefficient Measurement by a Simple

^{1}H NMR Method. *ACS Omega*, *2* (9), 6244–6249, (2017). https://doi.org/10.1021/acsomega.7b01102.

(59) Alpert, A. J. Hydrophilic-Interaction Chromatography for the Separation of Peptides, Nucleic Acids and Other Polar Compounds. *Journal of Chromatography A*, *499* (C), 177–196, (1990). https://doi.org/10.1016/S0021-9673(00)96972-3.

(60) Nováková, L.; Douša, M. Moderni HPLC Separace a Teorie v Praxi I. 2013, pp 157–164.

(61) Buszewski, B.; Noga, S. Hydrophilic Interaction Liquid Chromatography (HILIC)-a Powerful Separation Technique. *Analytical and Bioanalytical Chemistry*, *402* (1), 231–247, (2012). https://doi.org/10.1007/s00216-011-5308-5.

(62) Kumar, A.; Heaton, J. C.; McCalley, D. V. Practical Investigation of the Factors That Affect the Selectivity in Hydrophilic Interaction Chromatography. *Journal of Chromatography A*, *1276*, 33–46, (2013). https://doi.org/10.1016/j.chroma.2012.12.037.

(63) Neue, U. D.; Hudalla, C. J.; Iraneta, P. C. Influence of Pressure on the Retention of Sugars in Hydrophilic Interaction Chromatography. *Journal of Separation Science*, *33* (6–7), 838–840, (2010). https://doi.org/10.1002/jssc.200900628.

(64) Dejaegher, B.; Vander Heyden, Y. HILIC Methods in Pharmaceutical Analysis. *Journal of Separation Science*, *33* (6–7), 698–715, (2010). https://doi.org/10.1002/jssc.200900742.

(65) Nguyen, H. P.; Schug, K. A. The Advantages of ESI-MS Detection in Conjunction with HILIC Mode Separations: Fundamentals and Applications. *Journal of Separation Science, 31* (9), 1465–1480, (2008). https://doi.org/10.1002/jssc.200700630.

(66) Kebarle, P.; Verkerk, U. H. On the Mechanism of Electrospray Mass Spectrometry. *Electrospray and MALDI Mass Spectrometry*, 3–63, (2010).

(67) Nováková, L.; Douša, M. Moderni HPLC Separace a Teorie v Praxi II. 2013.

(68) Bhardwaj, S. K.; Dwivedi, K.; Agarwal, D. D. A Review: HPLC Method Development and Validation. *International Journal of Analytical and Bioanalytical Chemistry, 5* (4), 76–81, (2015).

(69) Vidushi, Y.; Bharkatiya, M. Hplc Method Development and Validation: *A Review. Research Journal of Life Science, Bioinformatics, Pharmaceutical and Chemical Sciences*, *4* (4), 39–46, (2017). https://doi.org/10.7897/2230-8407.04407.

(70) Swartz, M. HPLC Detectors: A Brief Review. *Journal of Liquid Chromatography and Related Technologies*, *33* (9–12), 1130–1150, (2010). https://doi.org/10.1080/10826076.2010.484356.

(71) Sigma-Aldrich. Method Development & Optimization https://www.sigmaaldrich.com/deepweb/assets/sigmaaldrich/marketing/global/documents/201/658/dicas-de-desenvolvimento-de-metodo-e-otimizacoes.pdf.

(72) Chen, Y.; Guo, Z.; Wang, X.; Qiu, C. Sample Preparation. *Journal of Chromatography. A*, *1184* (1–2), 191–219, (2008). https://doi.org/10.1016/j.chroma.2007.10.026.

(73) Ramos, L. Critical Overview of Selected Contemporary Sample Preparation Techniques. *Journal of Chromatography A*, *1221*, 84–98, (2012). https://doi.org/10.1016/j.chroma.2011.11.011.

(74) Opekar, F.; Jelínek, I.; Rychlovský, P.; Plzák, Z. Základni Analytická Chemie. Univerzita Karlova v Praze 2003, p 208.

(75) Klamt, A. Conductor-like Screening Model for Real Solvents: A New Approach to the Quantitative Calculation of Solvation Phenomena. *Journal of Physical Chemistry*, *99* (7), 2224–2235, (1995). https://doi.org/10.1021/j100007a062.

(76) Zawadzki, M.; Paduszyński, K.; Królikowska, M.; Grzechnik, E. COSMO-RS Predicted 1-Octanol/Water Partition Coefficient as Useful Ion Descriptor for Predicting Phase Behavior of Aqueous Solutions of Ionic Liquids. *Journal of Molecular Liquids,* 307, (2020). https://doi.org/10.1016/j.molliq.2020.112914.

(77) Putnam, R.; Taylor, R.; Klamt, A.; Eckert, F.; Schiller, M. Prediction of Infinite Dilution Activity Coefficients Using COSMO-RS. *Industrial and Engineering Chemistry Research*, *42* (15), 3635–3641, (2003). https://doi.org/10.1021/ie020974v.

(78) Hernández-Bravo, R.; Miranda, A. D.; Martínez-Mora, O.; Domínguez, Z.; Martínez-Magadán, J. M.; García-Chávez, R.; Domínguez-Esquivel, J. M. Calculation of the Solubility Parameter by COSMO-RS Methods and Its Influence on Asphaltene-Ionic

Liquid Interactions. *Industrial and Engineering Chemistry Research*, *56* (17), 5107–5115, (2017). https://doi.org/10.1021/acs.iecr.6b05035.

(79) Klamt, A.; Jonas, V.; Bürger, T.; Lohrenz, J. C. W. Refinement and Parametrization of COSMO-RS. *Journal Physical Chemistry A*, *102* (26), 5074–5085, (1998). https://doi.org/10.1021/jp980017s.

(80) Wang, J.; Guo, Y.; Liu, F.; Zhang, X.; Wang, W.; Peng, Q. COSMO-RS Prediction and Experimental Verification of Deep Eutectic Solvents for Water Insoluble Pesticides with High Solubility. *Journal of Molecular Liquids*, *349*, 118139, (2022). https://doi.org/10.1016/j.molliq.2021.118139.

(81) Kurfiřt, M.; Dračínský, M.; Červenková Šťastná, L.; Cuřínová, P.; Hamala, V.; Hovorková, M.; Bojarová, P.; Karban, J. Selectively Deoxyfluorinated N-Acetyllactosamine Analogues as 19F NMR Probes to Study Carbohydrate-Galectin Interactions. *Chemistry - A European Journal*, *27* (51), 13040–13051, (2021). https://doi.org/10.1002/chem.202101752.

(82) Kartha, K. P. R.; Aloui, M.; Field, R. A. Iodine: A Versatile Reagent in Carbohydrate Chemistry III. Efficient Activation of Glycosyl Halides in Combination with DDQ1. *Tetrahedron Letters*, *37* (48), 8807–8810, (1996). https://doi.org/10.1016/S0040-4039(96)01995-8.

(83) Liu, Z.; Jenkinson, S. F.; Vermaas, T.; Adachi, I.; Wormald, M. R.; Hata, Y.; Kurashima, Y.; Kaji, A.; Yu, C. Y.; Kato, A.; Fleet, G. W. J. 3-Fluoroazetidinecarboxylic Acids and Trans,Trans- 3,4-Difluoroproline as Peptide Scaffolds: Inhibition of Pancreatic Cancer Cell Growth by a Fluoroazetidine Iminosugar. *Journal of Organic Chemistry*, *80* (9), 4244–4258, (2015). https://doi.org/10.1021/acs.joc.5b00463.

(84) Weisstein, E. Bessel's Correction https://mathworld.wolfram.com/BesselsCorrection.html.

(85) Kurfiřt, M.; Šťastná, L. Č.; Dračínský, M.; Pohl, R.; Císařová, I.; Jan, S.; Baka, M.; Hamala, V.; Canada, F. J.; Arda, A.; Jimenez-Barbero, J.; Karban, J. Influence of Selective Deoxyfluorination on the Molecular Structure of Type-2 N-Acetyllactosamine. *Journal of Organic Chemistry,* *89* (17), 11875-11890 (2024).

https://doi.org/10.1021/acs.joc.4c00879.

(86) St-Gelais, J.; Côté, É.; Lainé, D.; Johnson, P. A.; Giguère, D. Addressing the Structural Complexity of Fluorinated Glucose Analogues: Insight into Lipophilicities and Solvation Effects. *Chemistry - A European Journal*, *26* (59), 13499–13506, (2020). https://doi.org/10.1002/chem.202002825.

(87) Klamt, A.; Eckert, F.; Arlt, W. COSMO-RS: An Alternative to Simulation for Calculating Thermodynamic Properties of Liquid Mixtures. *Annual Review of Chemical and Biomolecular Engineering*, *1*, 101–122, (2010). https://doi.org/10.1146/annurev-chembioeng-073009-100903.